

An a posteriori error analysis based on equilibrated stresses for finite element approximations of frictional contact

Ilaria Fontana ^{*,1} and Daniele A. Di Pietro²

¹*Department of Engineering Sciences and Applied Mathematics,
Northwestern University, Evanston, IL 60208, USA*

²*IMAG, Univ Montpellier, CNRS, Montpellier, France*

Abstract

We consider the unilateral contact problem between an elastic body and a rigid foundation in a description that includes both Tresca and Coulomb friction conditions. For this problem, we present an a posteriori error analysis based on an equilibrated stress reconstruction in the Arnold–Falk–Winther space that includes a guaranteed upper bound distinguishing the different components of the error. This analysis is the starting point for the development of an adaptive algorithm including a stopping criterion for the generalized Newton method. This algorithm is then used to perform numerical simulations that validate the theoretical results.

Keywords: frictional unilateral contact problem, weakly enforced contact conditions, a posteriori error estimate, equilibrated stress reconstruction, Arnold–Falk–Winther mixed finite element, adaptive algorithms

MSC2020 classification: 74M15, 74S05, 65N15, 65N30, 65N50

1 Introduction

In the field of mechanical engineering, accounting for contact conditions with friction is indispensable for the accurate representation of the behavior of an elastic object. This is particularly crucial in structural studies, such as those involving dams, where ensuring safety demands a thorough analysis. The most frequently used friction conditions in mechanical problems are Tresca and Coulomb conditions. In this work, we consider the Tresca or Coulomb unilateral contact problems between an elastic body and a rigid foundation. Numerous techniques exist in the literature for approximating solutions to such problems, including penalty formulations [23], mixed formulations [19], and methods based on the weak enforcement of contact conditions à la Nitsche [7]. Since the original work on Dirichlet boundary conditions [24], Nitsche’s technique has been extended to general boundary conditions [22] and, more recently, to the unilateral contact problem without friction [9]; see [7] for a review including subsequent developments. From the numerical standpoint, this technique is appealing as it does not require the introduction of Lagrange multipliers and results in an easily implementable formulation. The starting point is the general formulation proposed in [1], which covers both Tresca and Coulomb friction cases.

*Corresponding author

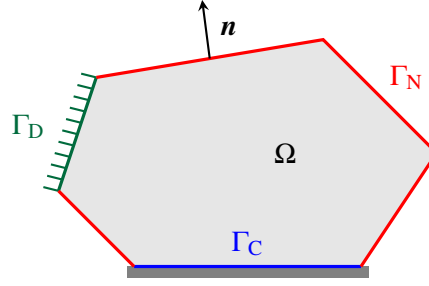


Figure 1: Example of domain Ω with $d = 2$. The boundary $\partial\Omega$ is subdivided into Γ_D (in green), Γ_N (in red), and Γ_C (in blue).

The primary focus of this paper is the extension of the a posteriori error analysis via equilibrated stress reconstruction developed in [14] to the frictional unilateral contact problem. This technique, presented in [16] for the Poisson problem, is based on the Prager–Synge inequality [25]. We provide a guaranteed upper bound of the dual norm of the error without using any saturation assumption, see Theorems 3 and 6 below. The presented upper bound is expressed in terms of fully computable a posteriori error estimators which distinguish the different sources of error. Besides the data of the problem (volumetric and surface loadings), these estimators involve the approximate solution \mathbf{u}_h and an equilibrated stress reconstruction $\boldsymbol{\sigma}_h$, i.e., an $\mathbb{H}(\mathbf{div})$ -conforming correction of the stress tensor $\boldsymbol{\sigma}(\mathbf{u}_h)$ locally in equilibrium with the force source terms.

The paper is organized as follows. In Section 2, we introduce the frictional unilateral contact problem in both strong and weak forms, along with its discretization à la Nitsche. Additionally, we provide the main space-related and mesh-related notations that we will use throughout the rest of the paper in Tables 1 and 2. Section 3 showcases the main results of the work: a basic a posteriori error estimate, a refined version distinguishing the components of the error, and an adaptive algorithm based on the latter. This algorithm includes an adaptive stopping criterion for the linearization iterations. Moreover, we compare the dual norm of the residual with the energy norm. In Section 4 we explicitly propose how to construct an equilibrated stress reconstruction with the right properties by assembling the solutions of local problems on element patches around mesh vertices. Section 5 validates the results of Section 3 with two numerical examples with Tresca and Coulomb friction conditions, respectively. Finally, Section 6 concludes the work by presenting results of local and global efficiency.

2 Setting

2.1 Continuous problem

We consider a domain $\Omega \in \mathbb{R}^d$, $d \in \{2, 3\}$, which represents a body with elastic behavior, and we suppose for simplicity that Ω is a polygon if $d = 2$ or a polyhedron if $d = 3$, so that it can be covered exactly by a finite element mesh. The boundary of the domain is denoted by $\partial\Omega$ and is subdivided into three nonoverlapping parts: Γ_D , Γ_N , and Γ_C (see Figure 1 for a two-dimensional example) such that $|\Gamma_D| > 0$ and $|\Gamma_C| > 0$, where $|\cdot|$ is the Hausdorff measure. The setting of the problem is the following: the body is clamped at Γ_D , it is subject to volumetric forces $\mathbf{f} \in L^2(\Omega)$ in Ω and to surface forces $\mathbf{g}_N \in L^2(\Gamma_N)$ on the portion of the boundary Γ_N , in the reference configuration it is in contact with a rigid foundation on Γ_C , while in the deformed configuration the contact region is included in Γ_C . On the boundary $\partial\Omega$, we consider the outward unit normal vector \mathbf{n} that allows us to decompose any displacement field \mathbf{v} and any density of surface force $\boldsymbol{\sigma}(\mathbf{v})\mathbf{n}$ into their normal

and tangential components:

$$\mathbf{v} = v^n \mathbf{n} + \mathbf{v}^t \quad \text{and} \quad \boldsymbol{\sigma}(\mathbf{v})\mathbf{n} = \sigma^n(\mathbf{v})\mathbf{n} + \boldsymbol{\sigma}^t(\mathbf{v}). \quad (2.1)$$

The frictional unilateral contact problem then reads: Find the displacement $\mathbf{u} : \Omega \rightarrow \mathbb{R}^d$ such that

$$\mathbf{div} \boldsymbol{\sigma}(\mathbf{u}) + \mathbf{f} = \mathbf{0} \quad \text{in } \Omega, \quad (2.2a)$$

$$\boldsymbol{\sigma}(\mathbf{u}) = \lambda \operatorname{tr} \boldsymbol{\varepsilon}(\mathbf{u}) \mathbf{I}_d + 2\mu \boldsymbol{\varepsilon}(\mathbf{u}) \quad \text{in } \Omega, \quad (2.2b)$$

$$\mathbf{u} = \mathbf{0} \quad \text{on } \Gamma_D, \quad (2.2c)$$

$$\boldsymbol{\sigma}(\mathbf{u})\mathbf{n} = \mathbf{g}_N \quad \text{on } \Gamma_N, \quad (2.2d)$$

$$u^n \leq 0, \sigma^n(\mathbf{u}) \leq 0, \sigma^n(\mathbf{u}) u^n = 0 \quad \text{on } \Gamma_C, \quad (2.2e)$$

$$\begin{cases} |\boldsymbol{\sigma}^t(\mathbf{u})| \leq S(\mathbf{u}) & \text{if } \mathbf{u}^t = \mathbf{0} \\ \boldsymbol{\sigma}^t(\mathbf{u}) = -S(\mathbf{u}) \frac{\mathbf{u}^t}{|\mathbf{u}^t|} & \text{otherwise} \end{cases} \quad \text{on } \Gamma_C. \quad (2.2f)$$

Here, $\boldsymbol{\varepsilon}(\mathbf{v}) := \frac{1}{2}(\nabla \mathbf{v} + \nabla \mathbf{v}^\top)$ is the strain tensor field, $\boldsymbol{\sigma}(\mathbf{v}) \in \mathbb{R}_{\text{sym}}^{d \times d}$ is the Cauchy stress tensor, \mathbf{div} is the divergence operator acting row-wise on tensor valued functions, μ and λ denote the Lamé parameters, and $|\cdot|$ in (2.2f) is the Euclidian norm in \mathbb{R}^{d-1} .

The first contact condition (2.2e) is a complementary condition representing non-penetration ($u^n \leq 0$) and the absence of normal cohesive forces (if $u^n < 0$, then $\sigma^n(\mathbf{u}) = 0$). The second contact condition represents the friction condition and makes it possible to include in this formulation both Tresca and Coulomb models (see also [1]): $S(\mathbf{u}) = s \in L^2(\Gamma_C)$, $s \leq 0$, for the Tresca friction model, and $S(\mathbf{u}) = -\mu_{\text{Coul}} \sigma^n(\mathbf{u})$ for the Coulomb one, where $\mu_{\text{Coul}} \geq 0$ is the Coulomb friction coefficient. We remark that, while Tresca friction is easier to implement and analyze since the friction threshold s is a known function, Coulomb friction allows us to model the fact that there is no friction when the elastic body is not in contact with the rigid foundation in the deformed configuration.

Table 1 summarizes the main space-related notations used in the paper. In addition, we define the space $\mathbf{H}_D^1(\Omega)$ as the space of functions of $\mathbf{H}^1(\Omega)$ satisfying the homogeneous Dirichlet boundary condition (2.2c), and the space \mathbf{K} of admissible displacement:

$$\mathbf{H}_D^1(\Omega) := \{\mathbf{v} \in \mathbf{H}^1(\Omega) : \mathbf{v} = \mathbf{0} \text{ on } \Gamma_D\}, \quad \mathbf{K} := \{\mathbf{v} \in \mathbf{H}_D^1(\Omega) : v^n \leq 0 \text{ on } \Gamma_C\}.$$

The weak formulation of the problem (2.2) is the following variational inequality (see, e.g. [19, 7]): Find $\mathbf{u} \in \mathbf{K}$ such that

$$a(\mathbf{u}, \mathbf{v} - \mathbf{u}) + j(\mathbf{u}; \mathbf{v}) - j(\mathbf{u}; \mathbf{u}) \geq L(\mathbf{v} - \mathbf{u}) \quad \forall \mathbf{v} \in \mathbf{K}, \quad (2.3)$$

where

$$a(\mathbf{w}, \mathbf{v}) := (\boldsymbol{\sigma}(\mathbf{u}), \boldsymbol{\varepsilon}(\mathbf{v})), \quad L(\mathbf{v}) := (\mathbf{f}, \mathbf{v}) + (\mathbf{g}_N, \mathbf{v})_{\Gamma_N}, \quad (2.4)$$

$$j(\mathbf{u}; \mathbf{v}) := (S(\mathbf{u}), |\mathbf{v}^t|)_{\Gamma_C}. \quad (2.5)$$

for all $(\mathbf{u}, \mathbf{v}) \in \mathbf{H}^1(\Omega) \times \mathbf{H}^1(\Omega)$. It is known that this formulation has a unique solution for Tresca friction, while for Coulomb friction the analysis is more intricate. We refer to [1] and the references therein for a discussion.

Notation	Definition
X	Measurable set of \mathbb{R}^d or \mathbb{R}^{d-1} , typically: Ω , a portion of $\partial\Omega$, or the union of a finite subset of mesh elements
$H^s(X)$	Sobolev space of index s on D
$\mathbf{H}^s(X)$	Vector Sobolev space $[H^s(X)]^d$
$\mathbb{H}^s(X)$	Tensor Sobolev space $[H^s(X)]^{d \times d}$
$L^2(X)$	Sobolev space $H^0(D)$ of square-integrable functions on X
$\mathbf{L}^2(X)$	Vector space $[L^2(X)]^d$ or $[L^2(X)]^{d-1}$
$\mathbb{L}^2(X)$	Tensor space $[L^2(X)]^{d \times d}$
$\ \cdot\ _{s,X}$	Norm of $H^s(X)$ or $\mathbf{H}^s(X)$ according to the argument
$\ \cdot\ _X$	Norm of $L^2(X)$, $\mathbf{L}^2(X)$ or $\mathbb{L}^2(X)$ according to the argument
$\ \cdot\ $	Norm of $L^2(\Omega)$, $\mathbf{L}^2(\Omega)$ or $\mathbb{L}^2(\Omega)$ according to the argument
$(\cdot, \cdot)_X$	Inner product of $L^2(X)$, $\mathbf{L}^2(X)$ or $\mathbb{L}^2(X)$ according to the argument
(\cdot, \cdot)	Inner product of $L^2(\Omega)$, $\mathbf{L}^2(\Omega)$ or $\mathbb{L}^2(\Omega)$ according to the argument
$\mathbb{H}(\mathbf{div}, \Omega)$	Space spanned by functions of $\mathbb{L}^2(\Omega)$ with weak (row-wise) divergence in $\mathbf{L}^2(\Omega)$

Table 1: Space-related notations.

2.2 Discrete problem

We consider now a family $\{\mathcal{T}_h\}_h$ of conforming triangulations of Ω , indexed by the mesh size $h := \max_{T \in \mathcal{T}_h} h_T$, where h_T is the diameter of the element T . This family is assumed to be regular in the classical sense; see, e.g., [11, Eq. (3.1.43)]. Furthermore, each triangulation is conformal to the subdivision of the boundary into Γ_D , Γ_N , and Γ_C in the sense that the interior of a boundary edge (if $d = 2$) or face (if $d = 3$) cannot have a non-empty intersection with more than one part of the subdivision. Mesh-related notations that will be used in the a posteriori error analysis are collected in Table 2. For the sake of simplicity, from this point on we adopt the three-dimensional terminology and speak of faces instead of edges also in dimension $d = 2$.

For any $X \in \mathcal{T}_h \cup \mathcal{F}_h$ mesh element or face, $\mathcal{P}^n(X)$ is the space of d -variate polynomials of total degree $\leq n$ defined on X , and we set $\mathcal{P}^n(X) := [\mathcal{P}^n(X)]^d$ and $\mathbb{P}^n(X) := [\mathcal{P}^n(X)]^{d \times d}$. We will seek the approximate solution in the standard Lagrange finite element space of degree $p \geq 1$ with strongly enforced boundary condition on Γ_D :

$$\mathbf{V}_h := \{v_h \in \mathbf{H}_D^1(\Omega) : v_h|_T \in \mathcal{P}^p(T) \text{ for any } T \in \mathcal{T}_h\}. \quad (2.6)$$

The key idea of the method we focus on consists in rewriting the contact boundary conditions (2.2e) and (2.2f) in a compact way and enforcing them à la Nitsche. For this purpose, we introduce the projector $[x]_{\mathbb{R}^-} = \frac{1}{2}(x - |x|)$ on the half-line of negative numbers \mathbb{R}^- , and the orthogonal projector $[\mathbf{x}]_\alpha: \mathbb{R}^{d-1} \rightarrow \mathbb{R}^{d-1}$ on the $(d-1)$ -dimensional ball $B(\mathbf{0}, \alpha)$ centered in $\mathbf{0}$ with radius $\alpha > 0$, i.e.,

$$[\mathbf{x}]_\alpha = \begin{cases} \mathbf{x} & \text{if } |\mathbf{x}| \leq \alpha, \\ \alpha \frac{\mathbf{x}}{|\mathbf{x}|} & \text{otherwise.} \end{cases} \quad (2.7)$$

In addition, for every real number θ and every positive bounded function $\gamma: \Gamma_C \rightarrow \mathbb{R}^+$, we define

Notation	Definition
\mathcal{F}_h	Set of faces of \mathcal{T}_h
\mathcal{F}_h^b	Set of boundary faces, i.e., $\{F \in \mathcal{F}_h : F \subset \partial\Omega\}$
$\mathcal{F}_h^D \cup \mathcal{F}_h^N \cup \mathcal{F}_h^C$	Partition of \mathcal{F}_h^b induced by the boundary and contact conditions
\mathcal{F}_h^i	Set of interior faces, i.e., $\mathcal{F}_h \setminus \mathcal{F}_h^b$
\mathcal{F}_T	Set of faces of the element $T \in \mathcal{T}_h$, i.e., $\{F \in \mathcal{F}_h : F \subset \partial T\}$
$\mathcal{F}_T^\bullet, \bullet \in \{b, D, N, C\}$	$\mathcal{F}_T \cap \mathcal{F}_h^\bullet, T \in \mathcal{T}_h$
\mathcal{V}_h	Set of all the vertices of \mathcal{T}_h
\mathcal{V}_h^b	Set of boundary vertices, i.e., $\{\mathbf{a} \in \mathcal{V}_h : \mathbf{a} \in \partial\Omega\}$
\mathcal{V}_h^i	Set of interior vertices, i.e., $\mathcal{V}_h \setminus \mathcal{V}_h^b$
\mathcal{V}_T	Set of vertices of the element $T \in \mathcal{T}_h$, i.e., $\{\mathbf{a} \in \mathcal{V}_h : \mathbf{a} \in \partial T\}$
\mathcal{V}_F	Set of vertices of the mesh face $F \in \mathcal{F}_h$, i.e., $\{\mathbf{a} \in \mathcal{V}_h : \mathbf{a} \in \partial F\}$
\mathcal{V}_h^D	Set of Dirichlet boundary vertices, i.e., $\{\mathbf{a} \in \mathcal{V}_h : \mathbf{a} \in F, F \in \mathcal{F}_h^D\}$
ω_a	Union of the elements sharing the vertex $\mathbf{a} \in \mathcal{V}_h$, i.e., $\bigcup_{T \in \mathcal{T}_h, \mathbf{a} \in \partial T} T$

Table 2: Mesh-related notations.

the following linear operators [7]:

$$P_{\theta, \gamma}^n : \mathbf{W} \rightarrow L^2(\Gamma_C) \quad \text{and} \quad \mathbf{P}_{\theta, \gamma}^t : \mathbf{W} \rightarrow L^2(\Gamma_C) \quad (2.8)$$

$$\mathbf{v} \mapsto \theta \sigma^n(\mathbf{v}) - \gamma v^n, \quad \mathbf{v} \mapsto \theta \sigma^t(\mathbf{v}) - \gamma v^t,$$

where $\mathbf{W} := \{\mathbf{v} \in \mathbf{H}^1(\Omega) : \sigma(\mathbf{v})\mathbf{n}|_{\Gamma_C} \in L^2(\Gamma_C)\}$ (notice that $\mathbf{V}_h \subset \mathbf{W}$). Assuming that $\mathbf{u} \in \mathbf{W}$, the two contact conditions (2.2e) and (2.2f) can be rewritten as follows (see [12, 9, 10]):

$$\sigma^n(\mathbf{u}) = [\sigma^n(\mathbf{u}) - \gamma u^n]_{\mathbb{R}^-} = \left[P_{1, \gamma}^n(\mathbf{u}) \right]_{\mathbb{R}^-}, \quad (2.9)$$

$$\sigma^t(\mathbf{u}) = [\sigma^t(\mathbf{u}) - \gamma u^t]_{S(\mathbf{u})} = \left[\mathbf{P}_{1, \gamma}^t(\mathbf{u}) \right]_{S(\mathbf{u})} \quad (2.10)$$

From now on, we assume that γ is the positive piecewise constant function on Γ_C which satisfies: For all $T \in \mathcal{T}_h$ such that $|\partial T \cap \Gamma_C| > 0$,

$$\gamma|_{\partial T \cap \Gamma_C} = \frac{\gamma_0}{h_T},$$

where $\gamma_0 > 0$ is a fixed *Nitsche parameter*. Finally, we approximate the problem (2.2) with the following method [6]: Find $\mathbf{u}_h \in \mathbf{V}_h$ such that

$$a(\mathbf{u}_h, \mathbf{v}_h) - \left(\left[P_{1, \gamma}^n(\mathbf{u}_h) \right]_{\mathbb{R}^-}, v_h^n \right)_{\Gamma_C} - \left(\left[\mathbf{P}_{1, \gamma}^t(\mathbf{u}_h) \right]_{S_h(\mathbf{u}_h)}, v_h^t \right)_{\Gamma_C} = L(\mathbf{v}_h) \quad \forall \mathbf{v}_h \in \mathbf{V}_h, \quad (2.11)$$

where $S_h(\mathbf{u}_h)$ depends on the choice of $S(\mathbf{u})$: for the Tresca case $S_h(\mathbf{u}_h) = s$ while, for the Coulomb case, using again (2.9), $S_h(\mathbf{u}_h) = -\mu_{\text{Coul}} [P_{1, \gamma}^n(\mathbf{u}_h)]_{\mathbb{R}^-}$, see [1]. For further results concerning the existence and uniqueness of a solution we refer to [6, 10]. Notice that (2.11) is the non-symmetric variant of the Nitsche method corresponding to the choice $\theta = 0$ in the above references.

Remark 1 (Choice of normal contact conditions). In this work, we will focus on the unilateral contact problem with no jump on Γ_C between Ω and the rigid foundation, but it is also possible to adapt the present analysis to other cases by replacing the contact condition (2.2f):

- for the bilateral contact problem, we simply replace it with the condition $u^n = 0$;
- for the unilateral contact problem with normal gap g on Γ_C in the reference configuration, we replace it with the three conditions

$$u^n - g \leq 0, \sigma^n(\mathbf{u}) \leq 0, \sigma^n(\mathbf{u})(u^n - g) = 0. \quad (2.12)$$

In the first case, we do not need to introduce the projection operator $[\cdot]_{\mathbb{R}^-}$ and equation (2.9) becomes $\sigma^n(\mathbf{u}) = P_{1,\gamma}^n(\mathbf{u})$ while, in the second case, the definition of $P_{\theta,\gamma}^n$ has to be modified by replacing v^n with $v^n - g$.

3 A posteriori error analysis

The goal of this section is to present an a posteriori error estimate based on the notion of equilibrated stress reconstruction. In this framework, following the approach of [14], we measure the error associated with the approximate solution \mathbf{u}_h using the dual norm of a residual operator.

3.1 Basic a posteriori error estimate

Starting from the discrete problem (2.11) and denoting by $(\mathbf{H}_D^1(\Omega))^*$ the dual space of $\mathbf{H}_D^1(\Omega)$, for all discrete function $\mathbf{w}_h \in \mathbf{V}_h$, we define the *residual* $\mathcal{R}(\mathbf{w}_h) \in (\mathbf{H}_D^1(\Omega))^*$ by its action on the space $\mathbf{H}_D^1(\Omega)$:

$$\langle \mathcal{R}(\mathbf{w}_h), \mathbf{v} \rangle := L(\mathbf{v}) - a(\mathbf{w}_h, \mathbf{v}) + \left(\left[P_{1,\gamma}^n(\mathbf{w}_h) \right]_{\mathbb{R}^-}, v^n \right)_{\Gamma_C} + \left(\left[\mathbf{P}_{1,\gamma}^t(\mathbf{w}_h) \right]_{S_h(\mathbf{w}_h)}, \mathbf{v}_h^t \right)_{\Gamma_C} \quad (3.1)$$

for all $\mathbf{v} \in \mathbf{H}_D^1(\Omega)$. Here, $\langle \cdot, \cdot \rangle$ denotes the duality pairing between $\mathbf{H}_D^1(\Omega)$ and $(\mathbf{H}_D^1(\Omega))^*$. Let

$$\|\mathbf{v}\|^2 := \|\nabla \mathbf{v}\|^2 + |\mathbf{v}|_{C,h}^2 \quad \forall \mathbf{v} \in \mathbf{H}_D^1(\Omega), \quad (3.2)$$

with

$$|\mathbf{v}|_{C,h}^2 := \sum_{F \in \mathcal{F}_h^C} \frac{1}{h_F} \|\mathbf{v}\|_F^2 \quad \forall \mathbf{v} \in \mathbf{H}_D^1(\Omega). \quad (3.3)$$

Given $\mathbf{w}_h \in \mathbf{V}_h$, the dual norm of the residual $\mathcal{R}(\mathbf{w}_h)$ on the normed space $(\mathbf{H}_D^1(\Omega), \|\cdot\|)$ is given by

$$\|\mathcal{R}(\mathbf{w}_h)\|_* := \sup_{\mathbf{v} \in \mathbf{H}_D^1(\Omega), \|\mathbf{v}\|=1} \langle \mathcal{R}(\mathbf{w}_h), \mathbf{v} \rangle, \quad (3.4)$$

and the quantity $\|\mathcal{R}(\mathbf{u}_h)\|_*$ can be used as a measure of the error committed approximating the exact solution \mathbf{u} with \mathbf{u}_h .

Definition 2 (Equilibrated stress reconstruction). We will call *equilibrated stress reconstruction* any tensor-valued field $\sigma_h : \Omega \mapsto \mathbb{R}^{d \times d}$ such that:

1. $\sigma_h \in \mathbb{H}(\mathbf{div}, \Omega)$,
2. $(\mathbf{div} \sigma_h + \mathbf{f}, \mathbf{v})_T = 0$ for every $\mathbf{v} \in \mathcal{P}^0(T)$ and every $T \in \mathcal{T}_h$,

3. $(\boldsymbol{\sigma}_h \mathbf{n})|_F \in \mathbf{L}^2(F)$ for every $F \in \mathcal{F}_h^N \cup \mathcal{F}_h^C$ and $(\boldsymbol{\sigma}_h \mathbf{n}, \mathbf{v})_F = (\mathbf{g}_N, \mathbf{v})_F$ for every $\mathbf{v} \in \mathcal{P}^0(F)$ and every $F \in \mathcal{F}_h^N$.

Given an equilibrated stress reconstruction $\boldsymbol{\sigma}_h$, for every element $T \in \mathcal{T}_h$, we define the following local error estimators:

$$\begin{aligned} \eta_{\text{osc},T} &:= \frac{h_T}{\pi} \|\mathbf{f} + \mathbf{div} \boldsymbol{\sigma}_h\|_T, & (\text{oscillation}) \\ \eta_{\text{str},T} &:= \|\boldsymbol{\sigma}_h - \boldsymbol{\sigma}(\mathbf{u}_h)\|_T, & (\text{stress}) \\ \eta_{\text{Neu},T} &:= \sum_{F \in \mathcal{F}_T^N} C_{t,T,F} h_F^{1/2} \|\mathbf{g}_N - \boldsymbol{\sigma}_h \mathbf{n}\|_F, & (\text{Neumann}) \\ \eta_{\text{cnt},T} &:= \sum_{F \in \mathcal{F}_T^C} h_F^{1/2} \left\| \left[\mathbf{P}_{1,\gamma}^n(\mathbf{u}_h) \right]_{\mathbb{R}^-} - \boldsymbol{\sigma}_h^n \right\|_F, & (\text{normal contact}) \\ \eta_{\text{fric},T} &:= \sum_{F \in \mathcal{F}_T^C} h_F^{1/2} \left\| \left[\mathbf{P}_{1,\gamma}^t(\mathbf{u}_h) \right]_{S_h(\mathbf{u}_h)} - \boldsymbol{\sigma}_h^t \right\|_F, & (\text{friction}) \end{aligned}$$

where, $C_{t,T,F}$ is the constant of the trace inequality $\|\mathbf{v} - \bar{\mathbf{v}}_F\|_F \leq C_{t,T,F} h_F^{1/2} \|\nabla \mathbf{v}\|_T$ with $\bar{\mathbf{v}}_F := \frac{1}{|F|} \int_F \mathbf{v}$, valid for every $\mathbf{v} \in \mathbf{H}^1(T)$ and any $F \in \mathcal{F}_T$ (see [29, Theorem 4.6.3] or [13, Section 1.4]).

The estimator $\eta_{\text{osc},T}$ represents the residual of the volumetric force balance equation (2.2a) inside the element T , $\eta_{\text{str},T}$ the difference between the Cauchy stress tensor computed from \mathbf{u}_h and the equilibrated stress reconstruction, $\eta_{\text{Neu},T}$ the residual of the Neumann boundary condition (2.2d), $\eta_{\text{cnt},T}$ the residual of the normal condition (2.2e) on the contact boundary, and $\eta_{\text{fric},T}$ the residual of the friction condition.

The following result shows a guaranteed upper bound of the dual norm of the residual (3.1) based on these local estimators.

Theorem 3 (A posteriori error estimate for the dual norm of the residual). *Let \mathbf{u}_h be the solution of (2.11), $\mathcal{R}(\mathbf{u}_h)$ the residual defined by (3.1), and $\boldsymbol{\sigma}_h$ an equilibrated stress reconstruction in the sense of Definition 2. Then,*

$$\|\|\mathcal{R}(\mathbf{u}_h)\|\|_* \leq \left(\sum_{T \in \mathcal{T}_h} \left((\eta_{\text{osc},T} + \eta_{\text{str},T} + \eta_{\text{Neu},T})^2 + (\eta_{\text{cnt},T} + \eta_{\text{fric},T})^2 \right) \right)^{1/2}.$$

Proof. Using the regularity of $\boldsymbol{\sigma}_h$ and of its normal trace established by Properties 1. and 3. in Definition 2, the following integration by parts formula holds:

$$(\boldsymbol{\sigma}_h, \nabla \mathbf{v}) + (\mathbf{div} \boldsymbol{\sigma}_h, \mathbf{v}) - (\boldsymbol{\sigma}_h \mathbf{n}, \mathbf{v})_{\Gamma_N} - (\boldsymbol{\sigma}_h^n, \mathbf{v}^n)_{\Gamma_C} - (\boldsymbol{\sigma}_h^t, \mathbf{v}^t)_{\Gamma_C} = 0 \quad \forall \mathbf{v} \in \mathbf{H}_D^1(\Omega). \quad (3.5)$$

Now, fix $\mathbf{v} \in \mathbf{H}_D^1(\Omega)$ such that $\|\|\mathbf{v}\|\|^2 = \|\nabla \mathbf{v}\|^2 + |\mathbf{v}|_{C,h}^2 = 1$ and consider the argument of the supremum in the definition (3.4) of the dual norm of the residual. Expanding $L(\cdot)$ and $a(\cdot, \cdot)$ according to (2.4) in the definition (3.1) of the residual written for $\mathbf{v}_h = \mathbf{u}_h$ and summing (3.5) to the resulting expression, we obtain

$$\begin{aligned} \langle \mathcal{R}(\mathbf{u}_h), \mathbf{v} \rangle &= (\mathbf{f} + \mathbf{div} \boldsymbol{\sigma}_h, \mathbf{v}) + (\boldsymbol{\sigma}_h - \boldsymbol{\sigma}(\mathbf{u}_h), \nabla \mathbf{v}) + (\mathbf{g}_N - \boldsymbol{\sigma}_h \mathbf{n}, \mathbf{v})_{\Gamma_N} \\ &\quad + \left(\left[\mathbf{P}_{1,\gamma}^n(\mathbf{u}_h) \right]_{\mathbb{R}^-} - \boldsymbol{\sigma}_h^n, \mathbf{v}^n \right)_{\Gamma_C} + \left(\left[\mathbf{P}_{1,\gamma}^t(\mathbf{u}_h) \right]_{S_h(\mathbf{u}_h)} - \boldsymbol{\sigma}_h^t, \mathbf{v}^t \right)_{\Gamma_C} =: \mathfrak{I}_1 + \dots + \mathfrak{I}_5, \end{aligned}$$

where we have additionally used the symmetry of σ_h to replace $\varepsilon(\mathbf{v})$ with $\nabla \mathbf{v}$ in the second term. The first four terms can be treated as in [14, Theorem 4], obtaining

$$\begin{aligned}\mathfrak{I}_1 &\leq \sum_{T \in \mathcal{T}_h} \eta_{\text{osc},T} \|\nabla \mathbf{v}\|_T, & \mathfrak{I}_2 &\leq \sum_{T \in \mathcal{T}_h} \eta_{\text{str},T} \|\nabla \mathbf{v}\|_T, \\ \mathfrak{I}_3 &\leq \sum_{T \in \mathcal{T}_h} \eta_{\text{Neu},T} \|\nabla \mathbf{v}\|_T, & \mathfrak{I}_4 &\leq \sum_{T \in \mathcal{T}_h} \eta_{\text{cnt},T} |\mathbf{v}|_{C,T},\end{aligned}$$

where $|\cdot|_{C,T}$ is the local counterpart of the seminorm (3.3) on the element $T \in \mathcal{T}_h$ obtained replacing \mathcal{F}_h^C with \mathcal{F}_T^C in the sum. Let us consider the fifth term \mathfrak{I}_5 . Using the Cauchy-Schwarz inequality, we get

$$\begin{aligned}\mathfrak{I}_5 &\leq \sum_{T \in \mathcal{T}_h} \sum_{F \in \mathcal{F}_T^C} \left\| \left[\mathbf{P}_{1,\gamma}^t(\mathbf{u}_h) \right]_{S_h(\mathbf{u}_h)} - \sigma_h^t \right\|_F \|\mathbf{v}^t\|_F \\ &\leq \sum_{T \in \mathcal{T}_h} \sum_{F \in \mathcal{F}_T^C} h_F^{1/2} \left\| \left[\mathbf{P}_{1,\gamma}^t(\mathbf{u}_h) \right]_{S_h(\mathbf{u}_h)} - \sigma_h^t \right\|_F |\mathbf{v}|_{C,T} = \sum_{T \in \mathcal{T}_h} \eta_{\text{frc},T} |\mathbf{v}|_{C,T}.\end{aligned}$$

Combining the above results and using the Cauchy-Schwarz inequality and the definition of the norm $\|\cdot\|$ (3.2), we conclude

$$\begin{aligned}\|\mathcal{R}(\mathbf{u}_h)\|_* &\leq \sup_{\mathbf{v} \in \mathbf{H}_D^1(\Omega), \|\mathbf{v}\|=1} \left\{ \sum_{T \in \mathcal{T}_h} (\eta_{a,T} \|\nabla \mathbf{v}\|_T + \eta_{b,T} |\mathbf{v}|_{C,T}) \right\} \\ &\leq \sup_{\mathbf{v} \in \mathbf{H}_D^1(\Omega), \|\mathbf{v}\|=1} \left\{ \left(\sum_{T \in \mathcal{T}_h} ((\eta_{a,T})^2 + (\eta_{b,T})^2) \right)^{1/2} \left(\sum_{T \in \mathcal{T}_h} (\|\nabla \mathbf{v}\|_T^2 + |\mathbf{v}|_{C,T}^2) \right)^{1/2} \right\} \\ &= \left(\sum_{T \in \mathcal{T}_h} ((\eta_{\text{osc},T} + \eta_{\text{str},T} + \eta_{\text{Neu},T})^2 + (\eta_{\text{cnt},T} + \eta_{\text{frc},T})^2) \right)^{1/2},\end{aligned}$$

where, for sake of brevity, $\eta_{a,T} := \eta_{\text{osc},T} + \eta_{\text{str},T} + \eta_{\text{Neu},T}$ and $\eta_{b,T} := \eta_{\text{cnt},T} + \eta_{\text{frc},T}$ for all $T \in \mathcal{T}_h$. \square

3.2 Separating the error components

In order to find numerically the approximate solution \mathbf{u}_h , we apply an iterative method to the nonlinear problem (2.11). In particular, in this work we consider the ‘‘generalized Newton method’’, also employed in [7], where no special treatment is done to account for the fact the projection operators $[\cdot]_{\mathbb{R}^-}$ and $[\cdot]_{S_h(\mathbf{u}_h)}$ are not Gateaux-differentiable. At each Newton iteration $k \geq 1$, we have to solve the linear problem: Find $\mathbf{u}_h^k \in \mathbf{V}_h$ such that

$$a(\mathbf{u}_h^k, \mathbf{v}_h) - \left(P_{\text{lin}}^{n,k-1}(\mathbf{u}_h^k), \mathbf{v}_h^n \right)_{\Gamma_C} - \left(\mathbf{P}_{\text{lin}}^{t,k-1}(\mathbf{u}_h^k), \mathbf{v}_h^t \right)_{\Gamma_C} = L(\mathbf{v}_h) \quad \forall \mathbf{v}_h \in \mathbf{V}_h, \quad (3.6)$$

where the linearized operators are obtained setting

$$\begin{aligned}P_{\text{lin}}^{n,k-1}(\mathbf{w}_h) &:= \left[P_{1,\gamma}^n(\mathbf{u}_h^{k-1}) \right]_{\mathbb{R}^-} + \frac{\partial \left[P_{1,\gamma}^n(\mathbf{v}) \right]_{\mathbb{R}^-}}{\partial \mathbf{v}} \Big|_{\mathbf{v}=\mathbf{u}_h^{k-1}} \cdot (\mathbf{w}_h - \mathbf{u}_h^{k-1}) \\ &= \begin{cases} 0 & \text{if } P_{1,\gamma}^n(\mathbf{u}_h^{k-1}) \leq 0 \\ P_{1,\gamma}^n(\mathbf{w}_h) & \text{otherwise} \end{cases}\end{aligned} \quad (3.7)$$

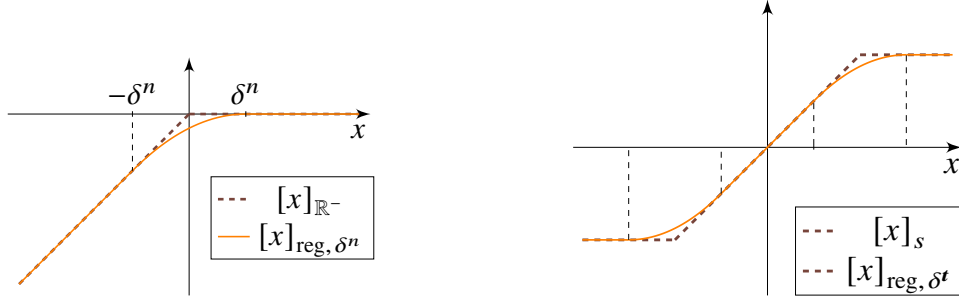


Figure 2: Regularized operators for $d = 2$ and constant Tresca friction.

and

$$\begin{aligned}
\mathbf{P}_{\text{lin}}^{\mathbf{t}, k-1}(\mathbf{w}_h) &:= \left[\mathbf{P}_{1,\gamma}^{\mathbf{t}}(\mathbf{u}_h^{k-1}) \right]_{S_h(\mathbf{u}_h^{k-1})} + \frac{\partial \left[\mathbf{P}_{1,\gamma}^{\mathbf{t}}(\mathbf{v}) \right]_{S_h(\mathbf{u}_h^{k-1})}}{\partial \mathbf{v}} \Big|_{\mathbf{v}=\mathbf{u}_h^{k-1}} \cdot (\mathbf{w}_h - \mathbf{u}_h^{k-1}) \\
&= \left[\mathbf{P}_{1,\gamma}^{\mathbf{t}}(\mathbf{u}_h^{k-1}) \right]_{S_h(\mathbf{u}_h^{k-1})} + \frac{\text{d} [x]_{S_h(\mathbf{u}_h^{k-1})}}{\text{d} \mathbf{x}} \Big|_{\mathbf{x}=\mathbf{P}_{1,\gamma}^{\mathbf{t}}(\mathbf{u}_h^{k-1})} \left(\mathbf{P}_{1,\gamma}^{\mathbf{t}}(\mathbf{w}_h) - \mathbf{P}_{1,\gamma}^{\mathbf{t}}(\mathbf{u}_h^{k-1}) \right).
\end{aligned} \tag{3.8}$$

Remark 4 (Possible regularization of projection operators). Another possible iterative approach consists in first regularizing the projection operators $[\cdot]_{\mathbb{R}^-}$ and $[\cdot]_{S_h(\mathbf{u}_h^{k-1})}$ and then applying the standard Newton method. For example, introducing two regularization parameters $\delta^n > 0$ and $\delta^t > 0$, we can define the regularized differentiable operators represented in Figure 2 for the case $d = 2$. In this work, for the sake of simplicity, we only consider the analysis without regularization and refer to [14] for a detailed treatment in the frictionless case.

Assumption 5 (Decomposition of the stress reconstruction). Let $\boldsymbol{\sigma}_h^k$ be an equilibrated stress reconstruction in the sense of Definition 2. Then, $\boldsymbol{\sigma}_h^k$ can be decomposed into two parts

$$\boldsymbol{\sigma}_h^k = \boldsymbol{\sigma}_{h,\text{dis}}^k + \boldsymbol{\sigma}_{h,\text{lin}}^k, \tag{3.9}$$

where $\boldsymbol{\sigma}_{h,\text{dis}}^k$ represents discretization and $\boldsymbol{\sigma}_{h,\text{lin}}^k$ represents linearization.

For an example of reconstruction that satisfies Assumption 5 we refer to Section 4. Now, we introduce the following local estimators that depend on the stress reconstruction and use its decomposition fixed by Assumption 5: For any mesh element $T \in \mathcal{T}_h$

$$\eta_{\text{osc},T}^k := \frac{h_T}{\pi} \|\mathbf{f} + \text{div } \boldsymbol{\sigma}_h^k\|_T, \tag{oscillation} \tag{3.10a}$$

$$\eta_{\text{str},T}^k := \|\boldsymbol{\sigma}_{h,\text{dis}}^k - \boldsymbol{\sigma}(\mathbf{u}_h^k)\|_T, \tag{stress} \tag{3.10b}$$

$$\eta_{\text{lin}1,T}^k := \|\boldsymbol{\sigma}_{h,\text{lin}}^k\|_T, \quad \eta_{\text{lin}2n,T}^k := \sum_{F \in \mathcal{F}_T^c} h_F^{1/2} \|\boldsymbol{\sigma}_{h,\text{lin}}^{k,n}\|_F, \tag{linearization} \tag{3.10c}$$

$$\eta_{\text{lin}2t,T}^k := \sum_{F \in \mathcal{F}_T^c} h_F^{1/2} \|\boldsymbol{\sigma}_{h,\text{lin}}^{k,t}\|_F$$

$$\eta_{\text{Neu},T}^k := \sum_{F \in \mathcal{F}_T^N} C_{t,T,F} h_F^{1/2} \|\mathbf{g}_N - \boldsymbol{\sigma}_h^k \mathbf{n}\|_F, \tag{Neumann} \tag{3.10d}$$

$$\eta_{\text{cnt},T}^k := \sum_{F \in \mathcal{F}_T^c} h_F^{1/2} \left\| \left[\mathbf{P}_{1,\gamma}^n(\mathbf{u}_h^k) \right]_{\mathbb{R}^-} - \sigma_{h,\text{dis}}^{k,n} \right\|_F. \quad (\text{contact}) \quad (3.10\text{e})$$

$$\eta_{\text{frc},T}^k := \sum_{F \in \mathcal{F}_T^c} h_F^{1/2} \left\| \left[\mathbf{P}_{1,\gamma}^t(\mathbf{u}_h^k) \right]_{S_h(\mathbf{u}_h^k)} - \sigma_{h,\text{dis}}^{k,t} \right\|_F, \quad (\text{friction}) \quad (3.10\text{f})$$

The corresponding global error estimators are defined by

$$\eta_{\bullet}^k := \left[\sum_{T \in \mathcal{T}_h} \left(\eta_{\bullet,T}^k \right)^2 \right]^{1/2}. \quad (3.11)$$

Theorem 6 (A posteriori error estimate distinguishing the error components). *Let $\mathbf{u}_h^k \in V_h$ be the solution of the linearized problem (3.6) with $\mathbf{P}_{\text{lin}}^{n,k-1}(\cdot)$ and $\mathbf{P}_{\text{lin}}^{t,k-1}$ defined by (3.7) and (3.8), respectively, and let $\mathcal{R}(\mathbf{u}_h^k)$ be the residual of \mathbf{u}_h^k defined by (3.1). Then, under Assumption 5, it holds*

$$\begin{aligned} & \|\mathcal{R}(\mathbf{u}_h^k)\|_* \\ & \leq \left[\sum_{T \in \mathcal{T}_h} \left((\eta_{\text{osc},T}^k + \eta_{\text{str},T}^k + \eta_{\text{lin}1,T}^k + \eta_{\text{Neu},T}^k)^2 + (\eta_{\text{cnt},T}^k + \eta_{\text{frc},T}^k + \eta_{\text{lin}2n,T}^k + \eta_{\text{lin}2t,T}^k)^2 \right) \right]^{1/2} \end{aligned} \quad (3.12)$$

and, as a result,

$$\|\mathcal{R}(\mathbf{u}_h^k)\|_* \leq \left[(\eta_{\text{osc}}^k + \eta_{\text{str}}^k + \eta_{\text{lin}1}^k + \eta_{\text{Neu}}^k)^2 + (\eta_{\text{cnt}}^k + \eta_{\text{frc}}^k + \eta_{\text{lin}2n}^k + \eta_{\text{lin}2t}^k)^2 \right]^{1/2}. \quad (3.13)$$

Proof. Proceeding as in the proof of Theorem 3, we obtain

$$\begin{aligned} & \|\mathcal{R}(\mathbf{u}_h^k)\|_* \\ & \leq \left\{ \sum_{T \in \mathcal{T}_h} \left[(\eta_{\text{osc},T}^k + \|\sigma_h^k - \sigma(\mathbf{u}_h^k)\|_T + \eta_{\text{Neu},T}^k)^2 + \left(\sum_{F \in \mathcal{F}_T^c} h_F^{1/2} \left\| \left[\mathbf{P}_{1,\gamma}^n(\mathbf{u}_h^k) \right]_{\mathbb{R}^-} - \sigma_h^{k,n} \right\|_F \right)^2 \right] \right\}^{1/2}. \end{aligned}$$

Then, decomposing σ_h^k into its discretization and linearization part according to (3.9), using the triangle inequality and the definition of the local estimators (3.10), we get (3.12). Finally, (3.13) is obtained from (3.12) applying twice the inequality $\sum_{T \in \mathcal{T}_h} (\sum_{i=1}^m a_{i,T})^2 \leq (\sum_{i=1}^m a_i)^2$ valid for all families of nonnegative real numbers $(a_{i,T})_{1 \leq i \leq m, T \in \mathcal{T}_h}$ with $a_i := \left(\sum_{T \in \mathcal{T}_h} a_{i,T}^2 \right)^{1/2}$ for all $1 \leq i \leq m$. \square

We close this section by introducing a fully adaptive algorithm for the refinement of an initial coarse mesh with a stopping criterion that automatically adjusts the number of Newton iterations at each mesh refinement iteration. With this goal, we fix a user-dependent parameter $\gamma_{\text{lin}} \in (0, 1)$ representing the relative magnitude of the linearization error with respect to the total error and define the linearization estimators

$$\eta_{\text{lin},T}^k := \eta_{\text{lin}1,T}^k + \sqrt{(\eta_{\text{lin}2n,T}^k)^2 + (\eta_{\text{lin}2t,T}^k)^2} \text{ for all } T \in \mathcal{T}_h \text{ and } \eta_{\text{lin}}^k := \left[\sum_{T \in \mathcal{T}_h} \left(\eta_{\text{lin},T}^k \right)^2 \right]^{1/2},$$

and, for $T \in \mathcal{T}_h$, the total estimator

$$\eta_{\text{tot},T}^k := \left[(\eta_{\text{osc},T}^k + \eta_{\text{str},T}^k + \eta_{\text{lin}1,T}^k + \eta_{\text{Neu},T}^k)^2 + (\eta_{\text{cnt},T}^k + \eta_{\text{frc},T}^k + \eta_{\text{lin}2n,T}^k + \eta_{\text{lin}2t,T}^k)^2 \right]^{1/2}. \quad (3.14)$$

Algorithm 1 Adaptive algorithm

- 1: **choose** an initial displacement $\mathbf{u}_h^0 \in \mathbf{V}_h$ and fix $\gamma_{\text{lin}} \in (0, 1)$
 - 2: **repeat** {mesh refinement}
 - 3: **set** $k = 0$
 - 4: **repeat** {Newton algorithm}
 - 5: **set** $\hat{k} = k + 1$
 - 6: **setup** the operators $P_{\text{lin},\delta}^{n,k-1}$ and $P_{\text{lin},\delta}^{t,k-1}$ and the linear system (3.6)
 - 7: **compute** $\mathbf{u}_h^k, \boldsymbol{\sigma}_h^k$, and the estimators (3.10)–(3.11)
 - 8: **until** $\eta_{\text{lin}}^k \leq \gamma_{\text{lin}} \left(\eta_{\text{osc}}^k + \eta_{\text{str}}^k + \eta_{\text{Neu}}^k + \eta_{\text{cnt}}^k + \eta_{\text{frc}}^k \right)$
 - 9: **refine** the elements of the mesh where $\eta_{\text{tot},T}^k$ is higher
 - 10: **until** $\eta_{\text{tot},T}^k$ is distributed evenly over the mesh
-

Remark 7 (Local stopping criterion). In the proposed algorithm, the stopping criterion for the number of Newton iterations is enforced in a global sense by comparing the size of the global linearization estimator with the sum of the other global estimators. It is also possible to introduce instead a local stopping criterion that has to be verified on all elements of the mesh:

$$\eta_{\text{lin},T}^k \leq \gamma_{\text{lin},T} \left(\eta_{\text{osc},T}^k + \eta_{\text{str},T}^k + \eta_{\text{Neu},T}^k + \eta_{\text{cnt},T}^k + \eta_{\text{frc},T}^k \right) \quad \forall T \in \mathcal{T}_h, \quad (3.15)$$

with $\gamma_{\text{lin},T} \in (0, 1)$ for all $T \in \mathcal{T}_h$. This criterion will be used in Section 6 to prove the local efficiency of the estimators (3.10).

3.3 Comparison with the energy norm

This subsection is devoted to comparing the dual norm of the residual $\|\mathcal{R}(\mathbf{u}_h)\|_*$ with the energy norm of the error $\|\mathbf{u} - \mathbf{u}_h\|_{\text{en}}$ defined in a standard way as

$$\|\mathbf{v}\|_{\text{en}}^2 := a(\mathbf{v}, \mathbf{v}) = (\boldsymbol{\sigma}(\mathbf{v}), \boldsymbol{\varepsilon}(\mathbf{v})) \quad \forall \mathbf{v} \in \mathbf{H}_D^1(\Omega). \quad (3.16)$$

In the following theorems, the notation $a \lesssim b$, $a, b \in \mathbb{R}$ will stand for $a \leq Cb$ where $C > 0$ is a constant independent of the mesh size h and of the Nitsche parameter γ_0 .

Theorem 8 (Control of the energy norm). *Assume that the solution \mathbf{u} of the continuous problem (2.2) belongs to $\mathbf{H}^{\frac{3}{2}+\nu}(\Omega)$ for some $\nu > 0$, and let $\mathbf{u}_h \in \mathbf{V}_h$ be the solution of the discrete problem (2.11). Then,*

$$\begin{aligned} \alpha^{1/2} \|\mathbf{u} - \mathbf{u}_h\|_{\text{en}} \lesssim & \|\mathcal{R}(\mathbf{u}_h)\|_* + \left(\sum_{F \in \mathcal{F}_h^c} \frac{1}{h_F} \left\| \boldsymbol{\sigma}^n(\mathbf{u}) - \left[P_{1,\gamma}^n(\mathbf{u}_h) \right]_{\mathbb{R}^-} \right\|_F^2 \right)^{1/2} \\ & + \left(\sum_{F \in \mathcal{F}_h^c} \frac{1}{h_F} \left\| \boldsymbol{\sigma}^t(\mathbf{u}) - \left[P_{1,\gamma}^t(\mathbf{u}_h) \right]_{S_h(\mathbf{u}_h)} \right\|_F^2 \right)^{1/2}, \end{aligned} \quad (3.17)$$

where α is the coercitivity constant of the bilinear form a (cf. (2.4)) such that $\alpha \|\mathbf{v}\|_{1,\Omega}^2 \leq \|\mathbf{v}\|_{\text{en}}^2$ for any $\mathbf{v} \in \mathbf{H}_D^1(\Omega)$.

Proof. Proceeding as in [14, Theorem 7], it is possible to show that

$$\begin{aligned} \|\mathbf{u} - \mathbf{u}_h\|_{\text{en}}^2 = & \langle \mathcal{R}(\mathbf{u}_h), \mathbf{u} - \mathbf{v}_h \rangle + \left(\boldsymbol{\sigma}^n(\mathbf{u}) - \left[P_{1,\gamma}^n(\mathbf{u}_h) \right]_{\mathbb{R}^-}, \mathbf{u}^n - \mathbf{u}_h^n \right)_{\Gamma_C} \\ & + \left(\boldsymbol{\sigma}^t(\mathbf{u}) - \left[P_{1,\gamma}^t(\mathbf{u}_h) \right]_{S_h(\mathbf{u}_h)}, \mathbf{u}^t - \mathbf{u}_h^t \right)_{\Gamma_C} =: \mathfrak{I}_1 + \mathfrak{I}_2 + \mathfrak{I}_3. \end{aligned} \quad (3.18)$$

For the first two terms we use, respectively, the definition (3.4) of the dual norm of the residual along with the coercivity of a and the Cauchy–Schwarz inequality followed by the definition (3.16) of $\|\cdot\|_{\text{en}}$ to obtain

$$\mathfrak{I}_1 \lesssim \alpha^{-1/2} \|\mathcal{R}(\mathbf{u}_h)\|_* \|\mathbf{u} - \mathbf{u}_h\|_{\text{en}} \quad (3.19)$$

$$\mathfrak{I}_2 \lesssim \alpha^{-1/2} \left(\sum_{F \in \mathcal{F}_h^C} \frac{1}{h_F} \left\| \sigma^n(\mathbf{u}) - [P_{1,\gamma}^n(\mathbf{u}_h)]_{\mathbb{R}^-} \right\|_F^2 \right)^{1/2} \|\mathbf{u} - \mathbf{u}_h\|_{\text{en}}. \quad (3.20)$$

For the remaining term, we apply Cauchy–Schwarz and trace inequalities to write:

$$\begin{aligned} \mathfrak{I}_3 &\lesssim \left(\sum_{F \in \mathcal{F}_h^C} \frac{1}{h_F} \left\| \sigma^t(\mathbf{u}) - [P_{1,\gamma}^t(\mathbf{u}_h)]_{S_h(\mathbf{u}_h)} \right\|_F^2 \right)^{1/2} \|\mathbf{u} - \mathbf{u}_h\|_{1,\Omega} \\ &\lesssim \alpha^{-1/2} \left(\sum_{F \in \mathcal{F}_h^C} \frac{1}{h_F} \left\| \sigma^t(\mathbf{u}) - [P_{1,\gamma}^t(\mathbf{u}_h)]_{S_h(\mathbf{u}_h)} \right\|_F^2 \right)^{1/2} \|\mathbf{u} - \mathbf{u}_h\|_{\text{en}}. \end{aligned} \quad (3.21)$$

We conclude by inserting the estimates (3.19), (3.20), and (3.21) into (3.18). \square

Theorem 9 (Control of the dual norm of the residual). *Assume that the solution \mathbf{u} of the continuous problem (2.2) belongs to $\mathbf{H}^{\frac{3}{2}+\nu}(\Omega)$ for some $\nu > 0$, and let $\mathbf{u}_h \in \mathbf{V}_h$ be the solution of the discrete problem (2.11). Then, it holds*

$$\begin{aligned} \|\mathcal{R}(\mathbf{u}_h)\|_* &\leq (d\lambda + 4\mu)^{1/2} \|\mathbf{u} - \mathbf{u}_h\|_{\text{en}} + \left(\sum_{F \in \mathcal{F}_h^C} h_F \left\| \sigma^n(\mathbf{u}) - [P_{1,\gamma}^n(\mathbf{u}_h)]_{\mathbb{R}^-} \right\|_F^2 \right)^{1/2} \\ &\quad + \left(\sum_{F \in \mathcal{F}_h^C} h_F \left\| \sigma^t(\mathbf{u}) - [P_{1,\gamma}^t(\mathbf{u}_h)]_{S_h(\mathbf{u}_h)} \right\|_F^2 \right)^{1/2}. \end{aligned} \quad (3.22)$$

Proof. This result can be proved by using the definition of the residual (3.1), an integration by parts, the symmetry of the stress tensor, and Cauchy–Schwarz inequalities. Here, we report only the main steps and refer to [14, Theorem 10] for the remaining details. Expanding a and L according to (2.4) into the definition (3.1) of the residual written for $\mathbf{w}_h = \mathbf{u}_h$, we get

$$\begin{aligned} \langle \mathcal{R}(\mathbf{u}_h), \mathbf{v} \rangle &= (\sigma(\mathbf{u} - \mathbf{u}_h), \varepsilon(\mathbf{v})) - \left(\sigma^n(\mathbf{u}) - [P_{1,\gamma}^n(\mathbf{u}_h)]_{\mathbb{R}^-}, \mathbf{v}^n \right)_{\Gamma_C} \\ &\quad - \left(\sigma^t(\mathbf{u}) - [P_{1,\gamma}^t(\mathbf{u}_h)]_{S_h(\mathbf{u}_h)}, \mathbf{v}^t \right)_{\Gamma_C} \\ &\leq \|\sigma(\mathbf{u} - \mathbf{u}_h)\| \|\nabla \mathbf{v}\| + \sum_{F \in \mathcal{F}_h^C} h_F^{1/2} \left\| \sigma^n(\mathbf{u}) - [P_{1,\gamma}^n(\mathbf{u}_h)]_{\mathbb{R}^-} \right\|_F \frac{1}{h_F^{1/2}} \|\mathbf{v}\|_F \\ &\quad + \sum_{F \in \mathcal{F}_h^C} h_F^{1/2} \left\| \sigma^t(\mathbf{u}) - [P_{1,\gamma}^t(\mathbf{u}_h)]_{S_h(\mathbf{u}_h)} \right\|_F \frac{1}{h_F^{1/2}} \|\mathbf{v}\|_F \\ &\leq \left[(d\lambda + 4\mu)^{1/2} \|\mathbf{u} - \mathbf{u}_h\|_{\text{en}} + \left(\sum_{F \in \mathcal{F}_h^C} h_F \left\| \sigma^n(\mathbf{u}) - [P_{1,\gamma}^n(\mathbf{u}_h)]_{\mathbb{R}^-} \right\|_F^2 \right)^{1/2} \right] \\ &\quad + \left(\sum_{F \in \mathcal{F}_h^C} h_F \left\| \sigma^t(\mathbf{u}) - [P_{1,\gamma}^t(\mathbf{u}_h)]_{S_h(\mathbf{u}_h)} \right\|_F^2 \right)^{1/2} \|\mathbf{v}\|, \end{aligned}$$

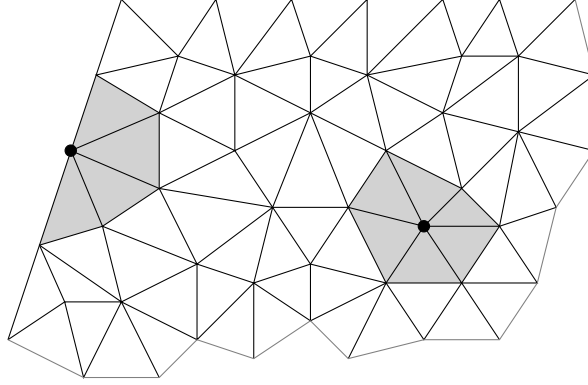


Figure 3: Illustration of a patch ω_a around an inner node $a \in \mathcal{V}_h^i$ and around a boundary node $a \in \mathcal{V}_h^b$.

Here, we have invoked the symmetry of $\sigma(\mathbf{u} - \mathbf{u}_h)$ to replace $\varepsilon(\mathbf{v})$ with $\nabla \mathbf{u}$ in the first term and then used Cauchy–Schwarz inequalities in the second step, and recalled the definitions (2.2b) of σ and (3.2) of $\|\cdot\|$ and used a Cauchy–Schwarz inequality on the sum to conclude. We obtain (3.22) applying the definition of dual norm (3.4). \square

Remark 10 (Terms depending on \mathbf{u}). The comparison results (3.17) and (3.22) contain two terms that depend on the exact solution \mathbf{u} . It should be possible to obtain similar bounds not containing these terms proceeding like in some recent work [5, 18]. In this paper, the results of Theorems 8 and 9 will be used in Section 5 for defining the two quantities (5.1) and (5.2) used as lower and upper bounds of the total estimator, respectively.

4 Equilibrated stress reconstruction

This section is devoted to describing the procedure to construct an equilibrated stress reconstruction satisfying the decomposition Assumption 5. In particular, σ_h^k is obtained working on patches of elements around the mesh vertices using the Arnold–Falk–Winther mixed finite element spaces [3]. We adapt the approach of [14] to the frictional contact problem modifying the definition of one of the spaces involved in the stress reconstruction.

First, we define, at the local level for any element $T \in \mathcal{T}_h$, the spaces

$$\Sigma_T := \mathbb{P}^p(T), \quad U_T := \mathcal{P}^{p-1}(T), \quad \Lambda_T := \{\boldsymbol{\mu} \in \mathbb{P}^{p-1}(T) : \boldsymbol{\mu} = -\boldsymbol{\mu}^T\}.$$

The corresponding global spaces are

$$\begin{aligned} \Sigma_h &:= \{\boldsymbol{\tau}_h \in \mathbb{H}(\mathbf{div}, \Omega) : \boldsymbol{\tau}_h|_T \in \Sigma_T \text{ for any } T \in \mathcal{T}_h\}, \\ U_h &:= \{\mathbf{v}_h \in \mathbf{L}^2(\Omega) : \mathbf{v}_h|_T \in U_T \text{ for any } T \in \mathcal{T}_h\}, \\ \Lambda_h &:= \{\boldsymbol{\mu}_h \in \mathbb{L}^2(\Omega) : \boldsymbol{\mu}_h|_T \in \Lambda_T \text{ for any } T \in \mathcal{T}_h\}. \end{aligned}$$

Then, for any vertex $a \in \mathcal{V}_h$ of the mesh, we consider the patch ω_a , see Figure 3, and we denote by \mathbf{n}_{ω_a} the outward normal unit vector on its boundary, with ψ_a the hat function associated with a and $\Sigma_h(\omega_a)$, $U_h(\omega_a)$, and $\Lambda_h(\omega_a)$ the restrictions of the spaces Σ_h , U_h and Λ_h to the patch ω_a .

At the patch level, we set

$$\begin{aligned}
\Sigma_h^a &:= \begin{cases} \{\tau_h \in \Sigma_h(\omega_a) : \tau_h \mathbf{n}_{\omega_a} = \mathbf{0} \text{ on } \partial\omega_a \setminus \Gamma_D\} & \text{if } a \in \mathcal{V}_h^b, \\ \{\tau_h \in \Sigma_h(\omega_a) : \tau_h \mathbf{n}_{\omega_a} = \mathbf{0} \text{ on } \partial\omega_a\} & \text{otherwise,} \end{cases} \\
\Sigma_{h,N,C,\bullet}^a &:= \begin{cases} \left\{ \begin{array}{l} \tau_h \in \Sigma_h(\omega_a) : \tau_h \mathbf{n}_{\omega_a} = \mathbf{0} \text{ on } \partial\omega_a \setminus \partial\Omega, \\ \tau_h \mathbf{n}_{\omega_a} = \mathbf{g}_\bullet \text{ on } \partial\omega_a \cap \Gamma_N, \text{ and} \\ \tau_h \mathbf{n}_{\omega_a} = \Pi_{\Sigma_h \mathbf{n}_{\omega_a}}(\psi_a \mathbf{P}_\bullet(\mathbf{u}_h^k)) \text{ on } \partial\omega_a \cap \Gamma_C \end{array} \right\} & \text{if } a \in \mathcal{V}_h^b, \\ \Sigma_h^a & \text{otherwise} \end{cases} \\
U_h^a &:= \begin{cases} U_h(\omega_a) & \text{if } a \in \mathcal{V}_h^D, \\ \{v_h \in U_h(\omega_a) : (v_h, z)_{\omega_a} = 0 \text{ for any } z \in \mathbf{RM}^d\} & \text{otherwise,} \end{cases} \\
\Lambda_h^a &:= \Lambda_h(\omega_a),
\end{aligned} \tag{4.1}$$

where $\bullet \in \{\text{dis}, \text{lin}\}$ and

$$\begin{aligned}
\mathbf{g}_{\text{dis}} &= \Pi_{\Sigma_h \mathbf{n}_{\omega_a}}(\psi_a \mathbf{g}_N) \quad \text{and} \quad \mathbf{g}_{\text{lin}} = \mathbf{0}, \\
\mathbf{P}_{\text{dis}}(\mathbf{u}_h^k) &:= \left[P_{1,\gamma}^n(\mathbf{u}_h^k) \right]_{\mathbb{R}^-} \mathbf{n} + \left[\mathbf{P}_{1,\gamma}^t(\mathbf{u}_h^k) \right]_{S_h(\mathbf{u}_h^k)},
\end{aligned} \tag{4.2}$$

$$\mathbf{P}_{\text{lin}}(\mathbf{u}_h^k) := \left(P_{\text{lin}}^{n,k-1}(\mathbf{u}_h^k) - \left[P_{1,\gamma}^n(\mathbf{u}_h^k) \right]_{\mathbb{R}^-} \right) \mathbf{n} + \mathbf{P}_{\text{lin}}^{t,k-1}(\mathbf{u}_h^k) - \left[\mathbf{P}_{1,\gamma}^t(\mathbf{u}_h^k) \right]_{S_h(\mathbf{u}_h^k)}, \tag{4.3}$$

and \mathbf{RM}^d is the space of rigid-body motions, i.e., $\mathbf{RM}^2 := \{\mathbf{b} + c(x_2, -x_1)^\top : \mathbf{b} \in \mathbb{R}^2, c \in \mathbb{R}\}$ and $\mathbf{RM}^3 := \{\mathbf{b} + \mathbf{c} \times \mathbf{x} : \mathbf{b}, \mathbf{c} \in \mathbb{R}^3\}$. Additionally, let $\mathbf{y}^{a,k} \in \mathbf{RM}^d$ be defined by

$$\begin{aligned}
(\mathbf{y}^{a,k}, \mathbf{z})_{\omega_a} &= (-\psi_a \mathbf{f} + \boldsymbol{\sigma}(\mathbf{u}_h^k) \nabla \psi_a, \mathbf{z})_{\omega_a} - (\Pi_{\Sigma_h \mathbf{n}_{\omega_a}}(\psi_a \mathbf{g}_N), \mathbf{z})_{\partial\omega_a \cap \Gamma_N} \\
&\quad - \left(\Pi_{\Sigma_h \mathbf{n}_{\omega_a}} \left(\psi_a \left(\left[P_{1,\gamma}^n(\mathbf{u}_h^k) \right]_{\mathbb{R}^-} \mathbf{n} + \left[\mathbf{P}_{1,\gamma}^t(\mathbf{u}_h^k) \right]_{S_h(\mathbf{u}_h^k)} \right) \right), \mathbf{z} \right)_{\partial\omega_a \cap \Gamma_C},
\end{aligned}$$

for all $\mathbf{z} \in \mathbf{RM}^d$ if $a \in \mathcal{V}_h^b$, and $\mathbf{y}^{a,k} = \mathbf{0}$ if $a \in \mathcal{V}_h^i$.

Remark 11 (Friction contact condition). Comparing this description with that provided in [14], we have modified the terms $\mathbf{P}_{\text{dis}}(\mathbf{u}_h^k)$ and $\mathbf{P}_{\text{lin}}(\mathbf{u}_h^k)$ defining the local spaces $\Sigma_{h,N,C,\text{dis}}^a$ and $\Sigma_{h,N,C,\text{lin}}^a$, respectively, to account for the friction contact conditions. These modifications will enable us to recover the properties of the stress reconstruction outlined in point 4. of Lemma 13, as will be discussed later. Additionally, they will facilitate the rewriting of the contact and friction estimator as (4.4c) and (4.4d), respectively.

Construction 12 (Equilibrated stress reconstruction distinguishing the error components).

Let, for $\bullet \in \{\text{dis}, \text{lin}\}$ and any vertex $a \in \mathcal{V}_h$, $(\boldsymbol{\sigma}_{h,\bullet}^{a,k}, \mathbf{r}_{h,\bullet}^{a,k}, \boldsymbol{\lambda}_{h,\bullet}^{a,k}) \in \Sigma_{h,N,C,\bullet}^a \times U_h^a \times \Lambda_h^a$ be the solution to the following problem:

$$\begin{aligned}
(\boldsymbol{\sigma}_{h,\bullet}^{a,k}, \boldsymbol{\tau}_h)_{\omega_a} + (\mathbf{r}_{h,\bullet}^{a,k}, \text{div } \boldsymbol{\tau}_h)_{\omega_a} + (\boldsymbol{\lambda}_{h,\bullet}^{a,k}, \boldsymbol{\tau}_h)_{\omega_a} &= (\boldsymbol{\tau}_{h,\bullet}^{a,k}, \boldsymbol{\tau}_h)_{\omega_a} \quad \forall \boldsymbol{\tau}_h \in \Sigma_h^a, \\
(\text{div } \boldsymbol{\sigma}_{h,\bullet}^{a,k}, \mathbf{v}_h)_{\omega_a} &= (\mathbf{v}_{h,\bullet}^{a,k}, \mathbf{v}_h)_{\omega_a} \quad \forall \mathbf{v}_h \in U_h^a, \\
(\boldsymbol{\sigma}_{h,\bullet}^{a,k}, \boldsymbol{\mu}_h)_{\omega_a} &= 0 \quad \forall \boldsymbol{\mu}_h \in \Lambda_h^a,
\end{aligned}$$

where

$$\boldsymbol{\tau}_{h,\bullet}^{a,k} := \begin{cases} \psi_a \boldsymbol{\sigma}(\mathbf{u}_h^k) & \text{if } \bullet = \text{dis}, \\ 0 & \text{if } \bullet = \text{lin}, \end{cases} \quad \mathbf{v}_{h,\bullet}^{a,k} := \begin{cases} -\psi_a \mathbf{f} + \boldsymbol{\sigma}(\mathbf{u}_h^k) \nabla \psi_a - \mathbf{y}^{a,k} & \text{if } \bullet = \text{dis}, \\ \mathbf{y}^{a,k} & \text{if } \bullet = \text{lin}. \end{cases}$$

Extending $\boldsymbol{\sigma}_{h,\bullet}^{a,k}$ by zero outside the patch ω_a , we set $\boldsymbol{\sigma}_{h,\bullet}^k := \sum_{a \in \mathcal{V}_h} \boldsymbol{\sigma}_{h,\bullet}^{a,k}$, and we define $\boldsymbol{\sigma}_h^k := \boldsymbol{\sigma}_{h,\text{dis}}^k + \boldsymbol{\sigma}_{h,\text{lin}}^k$.

By definition, $\mathbf{y}^{a,k}$ ensures that the forcing terms $\mathbf{v}_{h,\bullet}^{a,k}$ satisfy the following compatibility conditions for $\mathbf{a} \in \mathcal{V}_h^b \setminus \mathcal{V}_h^D$:

$$\begin{aligned} (\mathbf{v}_{h,\text{dis}}^{a,k}, \mathbf{z})_{\omega_a} &= (\Pi_{\Sigma_h n} \omega_a (\psi_a \mathbf{g}_N), \mathbf{z})_{\partial \omega_a \cap \Gamma_N} + \left(\Pi_{\Sigma_h n} \omega_a \psi_a \mathbf{P}_{\text{dis}}(\mathbf{u}_h^k), \mathbf{z} \right)_{\partial \omega_a \cap \Gamma_C}, \\ (\mathbf{v}_{h,\text{lin}}^{a,k}, \mathbf{z})_{\omega_a} &= \left(\Pi_{\Sigma_h n} \omega_a \psi_a \mathbf{P}_{\text{lin}}(\mathbf{u}_h^k), \mathbf{z} \right)_{\partial \omega_a \cap \Gamma_C} \end{aligned}$$

for any $\mathbf{z} \in \mathbf{RM}^d$, recalling that $\mathbf{P}_{\text{dis}}(\mathbf{u}_h^k)$ and $\mathbf{P}_{\text{lin}}(\mathbf{u}_h^k)$ are defined by (4.2) and (4.3), respectively. The obtained tensor $\boldsymbol{\sigma}_h^k$ is an equilibrated stress reconstruction in the sense of Definition 2 as stated by the following lemma.

Lemma 13 (Properties of $\boldsymbol{\sigma}_h^k$). *Let $\boldsymbol{\sigma}_h^k$ be defined by Construction 12. Then*

1. $\boldsymbol{\sigma}_{h,\text{dis}}^k, \boldsymbol{\sigma}_{h,\text{lin}}^k, \boldsymbol{\sigma}_h^k \in \mathbb{H}(\mathbf{div}, \Omega)$;
2. For every $T \in \mathcal{T}_h$ and every $\mathbf{v}_T \in \mathcal{P}^{p-1}(T)$, $(\mathbf{div} \boldsymbol{\sigma}_h^k + \mathbf{f}, \mathbf{v}_T)_T = 0$;
3. For every $F \in \mathcal{F}_h^N$ and every $\mathbf{v}_F \in \mathcal{P}^p(F)$, $(\boldsymbol{\sigma}_h^k \mathbf{n}, \mathbf{v}_F)_F = (\mathbf{g}_N, \mathbf{v}_F)_F$;
4. For every $F \in \mathcal{F}_h^C$ and every $\mathbf{v}_F \in \mathcal{P}^p(F)$,

$$\begin{aligned} (\boldsymbol{\sigma}_{h,\text{dis}}^{k,n}, \mathbf{v}_F^n)_F &= \left(\left[P_{1,\gamma}^n(\mathbf{u}_h^k) \right]_{\mathbb{R}^-}, \mathbf{v}_F^n \right)_F, & (\boldsymbol{\sigma}_{h,\text{dis}}^{k,t}, \mathbf{v}_F^t)_F &= \left(\left[\mathbf{P}_{1,\gamma}^t(\mathbf{u}_h^k) \right]_{S_h(\mathbf{u}_h^k)}, \mathbf{v}_F^t \right)_F, \\ (\boldsymbol{\sigma}_{h,\text{lin}}^{k,n}, \mathbf{v}_F^n)_F &= \left(P_{\text{lin}}^{n,k-1}(\mathbf{u}_h^k) - \left[P_{1,\gamma}^n(\mathbf{u}_h^k) \right]_{\mathbb{R}^-}, \mathbf{v}_F^n \right)_F, \end{aligned}$$

and

$$(\boldsymbol{\sigma}_{h,\text{lin}}^{k,t}, \mathbf{v}_F^t)_F = \left(P_{\text{lin}}^{k-1,t}(\mathbf{u}_h^k) - \left[\mathbf{P}_{1,\gamma}^t(\mathbf{u}_h^k) \right]_{S_h(\mathbf{u}_h^k)}, \mathbf{v}_F^t \right)_F.$$

Proof. For the proof of 1.–3., the arguments of [14, Lemma 16] can be easily adapted here. We focus on the proof of 4. Let $F \in \mathcal{F}_h^C$ and let $\mathbf{v}_F \in \mathcal{P}^p(F) = (\boldsymbol{\Sigma}_h \mathbf{n})|_F$. Then, applying the definition (4.1) of $\boldsymbol{\Sigma}_{h,N,C,\bullet}^a$, we get, for $\bullet \in \{\text{dis}, \text{lin}\}$,

$$(\boldsymbol{\sigma}_{h,\bullet}^k \mathbf{n}, \mathbf{v}_F)_F = \sum_{a \in \mathcal{V}_F} (\boldsymbol{\sigma}_{h,\bullet}^{a,k} \mathbf{n}, \mathbf{v}_F)_F = \sum_{a \in \mathcal{V}_F} \left(\psi_a \mathbf{P}_\bullet(\mathbf{u}_h^k), \mathbf{v}_F \right)_F = \left(\mathbf{P}_\bullet(\mathbf{u}_h^k), \mathbf{v}_F \right)_F,$$

where we have used the fact that $\sum_a \in \mathcal{V}_F \psi_a(\mathbf{x}) = 1$ for any $\mathbf{x} \in F$ to conclude. Point 4. follows using the decomposition into normal and tangential components and observing that, by the definitions (4.2) of \mathbf{P}_{dis} and (4.3) of \mathbf{P}_{lin} ,

$$\begin{aligned} P_{\text{dis}}^n(\mathbf{u}_h^k) &= \left[P_{1,\gamma}^n(\mathbf{u}_h^k) \right]_{\mathbb{R}^-}, & \mathbf{P}_{\text{dis}}^t(\mathbf{u}_h^k) &= \left[\mathbf{P}_{1,\gamma}^t(\mathbf{u}_h^k) \right]_{S_h(\mathbf{u}_h^k)}, \\ P_{\text{lin}}^n(\mathbf{u}_h^k) &= P_{\text{lin}}^{n,k-1}(\mathbf{u}_h^k) - \left[P_{1,\gamma}^n(\mathbf{u}_h^k) \right]_{\mathbb{R}^-}, & \mathbf{P}_{\text{lin}}^t(\mathbf{u}_h^k) &= \mathbf{P}_{\text{lin}}^{k-1,t}(\mathbf{u}_h^k) - \left[\mathbf{P}_{1,\gamma}^t(\mathbf{u}_h^k) \right]_{S_h(\mathbf{u}_h^k)}. \quad \square \end{aligned}$$

Remark 14 (Alternative expressions of local estimators). Thanks to Lemma 13, we can rewrite the oscillation (3.10a), Neumann (3.10d), contact (3.10e), and friction (3.10f) estimators as follows:

$$\eta_{\text{osc},T}^k = \frac{h_T}{\pi} \left\| \mathbf{f} - \boldsymbol{\Pi}_T^{p-1} \mathbf{f} \right\|_T, \quad (4.4a)$$

$$\eta_{\text{Neu},T}^k = \sum_{F \in \mathcal{F}_T^C} C_{t,T,F} h_F^{1/2} \left\| \mathbf{g}_N - \boldsymbol{\Pi}_F^p \mathbf{g}_N \right\|_F, \quad (4.4b)$$

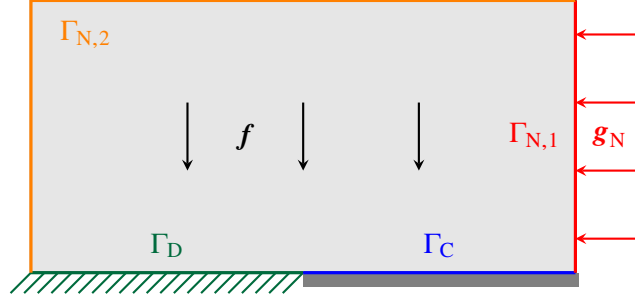


Figure 4: Rectangular domain of the numerical cases of Section 5.1 and 5.2 with representation of internal and lateral forces, and division of the domain's boundary. In particular, a uniform load \mathbf{g}_N is enforced on $\Gamma_{N,1}$, while homogeneous Neumann conditions are enforced on $\Gamma_{N,2}$. The portion of the boundary Γ_D is fixed, while contact is possible on Γ_C .

$$\eta_{\text{cnt},T}^k = \sum_{F \in \mathcal{F}_T^C} h_F^{1/2} \left\| \left[\mathbf{P}_{1,\gamma}^n(\mathbf{u}_h^k) \right]_{\mathbb{R}^-} - \Pi_F^P \left[\mathbf{P}_{1,\gamma}^n(\mathbf{u}_h^k) \right]_{\mathbb{R}^-} \right\|_F, \quad (4.4c)$$

$$\eta_{\text{fric},T}^k = \sum_{F \in \mathcal{F}_T^C} h_F^{1/2} \left\| \left[\mathbf{P}_{1,\gamma}^t(\mathbf{u}_h^k) \right]_{S_h(\mathbf{u}_h^k)} - \Pi_F^P \left[\mathbf{P}_{1,\gamma}^t(\mathbf{u}_h^k) \right]_{S_h(\mathbf{u}_h^k)} \right\|_F, \quad (4.4d)$$

where Π_T^{p-1} , Π_F^p , and Π_F^p denote the L^2 -orthogonal projectors on the polynomial spaces $\mathcal{P}^{p-1}(T)$, $\mathcal{P}^p(F)$, and $\mathcal{P}^p(F)$, respectively. Here, $\mathcal{P}^p(F)$ is either $[\mathcal{P}^p(F)]^d$ or $[\mathcal{P}^p(F)]^{d-1}$ depending on the context.

5 Numerical results

In this section, we present a panel of numerical results obtained applying Algorithm 1, using the open source finite element library FreeFem++ (see [20] and visit <https://freefem.org/> for details). With this flexible tool, we are able to implement the discrete problem (2.11) and compute the estimators (3.10)–(3.11) in a manner closely resembling their mathematical description. Specifically, the command `trunc` has been used to implement the local problems of Construction 12 in combination with the definition of hat function ψ_a . This command is also used to obtain sequences of uniformly refined meshes. Adaptive mesh refinement is, on the other hand, obtained using the `splitmesh`, ensuring that we automatically generate a conformal mesh satisfying the regularity requirements.

5.1 Tresca friction

Let $\Omega = (-1, 1) \times (0, 1)$ be a rectangular domain with the configuration represented in Figure 4, characterized by the following parameters: Young modulus $E = 1$ and Poisson ratio $\nu = 0.3$ (resulting in the Lamé coefficients $\mu \approx 0.385$ and $\lambda \approx 0.577$), a weight force $\mathbf{f} = (0, -0.02)$, a horizontal surface loading $\mathbf{g}_N = (-0.028, 0)$ on $\Gamma_{N,1}$ and $\mathbf{g}_N = \mathbf{0}$ on $\Gamma_{N,2}$. The Nitsche parameter is set to $\gamma_0 = 10E$, and Tresca friction conditions are enforced on the contact boundary portion Γ_C , i.e.,

$$\left[\mathbf{P}_{1,\gamma}^t(\mathbf{u}_h) \right]_{S_h(\mathbf{u}_h)} = \begin{cases} \mathbf{P}_{1,\gamma}^t(\mathbf{u}_h) & \text{if } |\mathbf{P}_{1,\gamma}^t(\mathbf{u}_h)| \leq s, \\ s \frac{\mathbf{P}_{1,\gamma}^t(\mathbf{u}_h)}{|\mathbf{P}_{1,\gamma}^t(\mathbf{u}_h)|} & \text{otherwise,} \end{cases}$$

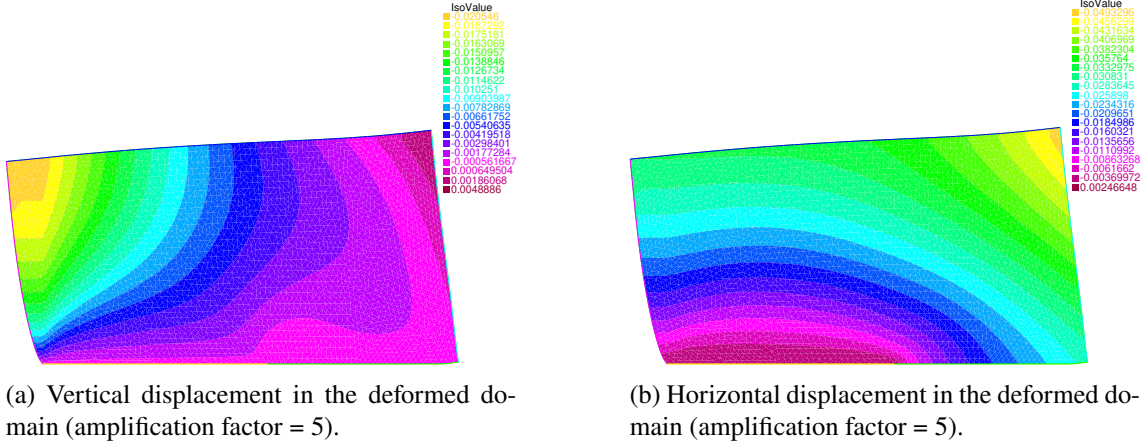


Figure 5: Vertical (*left*) and horizontal displacement (*right*) in the deformed configuration for the Tresca test case of Section 5.1.

with constant friction function defined as $s = 5 \cdot 10^{-3}$ on all Γ_C . For this problem, a closed-form solution is not available. Therefore, we adopt as reference solution the solution $\bar{\mathbf{u}}_h$ of the discrete problem (2.11) obtained using \mathcal{P}^2 Lagrange finite elements on a fine mesh with mesh size $h \approx 8.34 \cdot 10^{-3}$. The approximate solution \mathbf{u}_h is obtained using \mathcal{P}^1 Lagrange finite elements, and we employ the Newton method outlined in Subsection 3.2 for its computation. We remark that, although \mathcal{P}^1 finite elements are known to lock in the quasi-incompressible limit, it is admissible for the set of parameters considered here and it aligns with the use of the lowest-order mixed finite elements available in FreeFem++ for the computation of the equilibrated stress reconstructions described in Section 4. Figure 5b shows the vertical and horizontal displacement in the deformed configuration with an amplification factor equal to 5. In this configuration, the domain is in contact with the rigid foundation $y = 0$ in a non-empty interval I_C which is approximately $(0.035, 0.844)$.

In our adaptive approach, we base the refinement of the mesh on the distribution of the total local estimator $\eta_{\text{tot},T}$ (3.14), as stated by Algorithm 1. Here, for the sake of simplicity, we omit the superscript k . Starting with the initial coarse mesh in Figure 6a, after 4, 8, and 10 steps of adaptive spatial remeshing, we get the meshes shown in Figures 6b, 6c, and 6d, respectively. In this example, at least 6.2% of the elements are refined at each refinement iteration. Figure 6d shows that most of the refinement is along the contact boundary part Γ_C and at the endpoints of Γ_D , where two singularities arise due to the homogenous Dirichlet boundary conditions. In Figure 7a, we compare uniform and adaptive convergence focusing on the H^1 -norm $\|\bar{\mathbf{u}} - \mathbf{u}_h\|_{1,\Omega}$ and energy norm $\|\bar{\mathbf{u}} - \mathbf{u}_h\|_{\text{en}}$ defined by (3.16). As expected, the rate of convergence with respect to the number of degrees of freedom $\dim(\mathbf{V}_h)$ is better using the adaptive approach. Specifically, the asymptotic rates of convergence for the H^1 -norm and energy norms are approximately 0.328 and 0.282 in the uniform case, and 0.450 and 0.463 in the adaptive one. In Figure 7b, we visualize the value of the global total estimator constructed from the definition of the local total estimator (3.14) as

$$\eta_{\text{tot}} := \left(\sum_{T \in \mathcal{T}_h} (\eta_{\text{tot},T})^2 \right)^{1/2},$$

and we compare it with the following quantities defined from Theorem 8 and Theorem 9, respectively:

$$\mathcal{L}(\mathbf{u}_h) := \mu^{1/2} \|\bar{\mathbf{u}}_h - \mathbf{u}_h\|_{\text{en}} \quad (5.1)$$

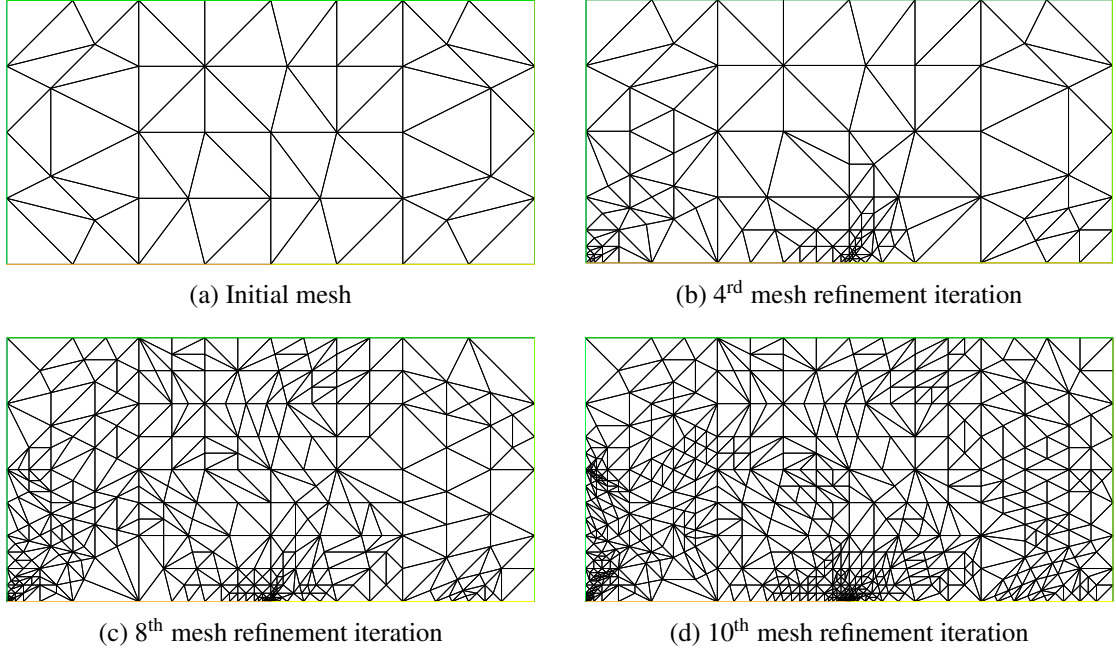


Figure 6: Initial mesh and adaptively refined mesh after 4, 8, and 10 remeshing steps, respectively, for the Tresca test case of Section 5.1.

and

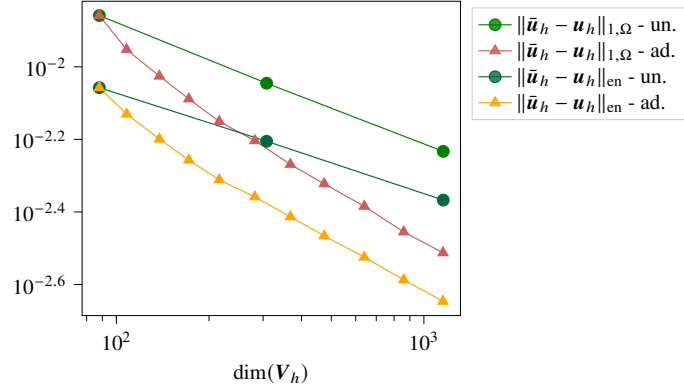
$$\begin{aligned}
\mathcal{U}(\mathbf{u}_h) := & (d\lambda + 4\mu)^{1/2} \|\bar{\mathbf{u}}_h - \mathbf{u}_h\|_{\text{en}} + \left(\sum_{F \in \mathcal{F}_h^C} h_F \left\| \boldsymbol{\sigma}^n(\bar{\mathbf{u}}_h) - \left[\mathbf{P}_{1,\gamma}^n(\mathbf{u}_h) \right]_{\mathbb{R}^-} \right\|_F^2 \right)^{1/2} \\
& + \left(\sum_{F \in \mathcal{F}_h^C} h_F \left\| \boldsymbol{\sigma}^t(\bar{\mathbf{u}}_h) - \left[\mathbf{P}_{1,\gamma}^t(\mathbf{u}_h) \right]_{S_h(\mathbf{u}_h)} \right\|_F^2 \right)^{1/2}. \tag{5.2}
\end{aligned}$$

The corresponding effectivity indices shown by Figure 7c are defined in the usual way:

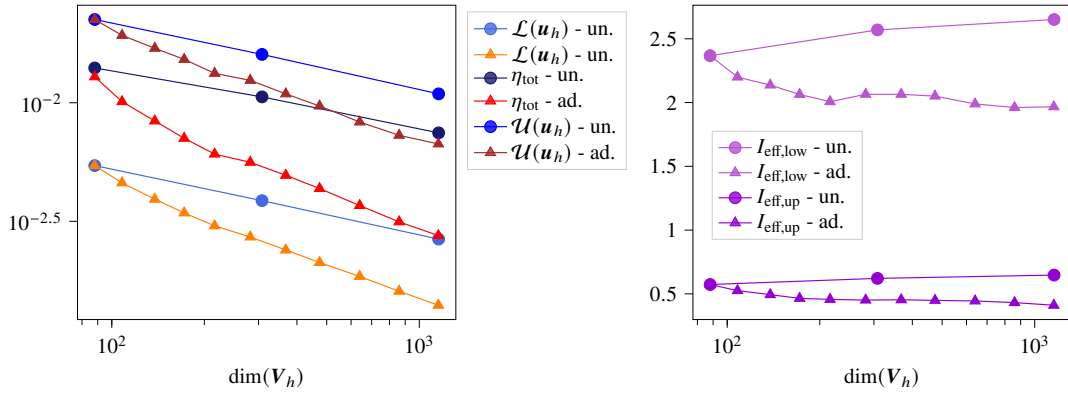
$$I_{\text{eff,low}} := \frac{\eta_{\text{tot}}}{\mathcal{L}(\mathbf{u}_h)} = \frac{\eta_{\text{tot}}}{\mu^{1/2} \|\bar{\mathbf{u}}_h - \mathbf{u}_h\|_{\text{en}}} \quad \text{and} \quad I_{\text{eff,up}} := \frac{\eta_{\text{tot}}}{\mathcal{U}(\mathbf{u}_h)}. \tag{5.3}$$

Notice that, for both the uniform and adaptive approaches, at the end of each mesh refinement iteration we get $\mathcal{L}(\mathbf{u}_h) < \eta_{\text{tot}} < \mathcal{U}(\mathbf{u}_h)$ or, equivalently $I_{\text{eff,low}} > 1$ and $I_{\text{eff,up}} < 1$, validating the results (3.17) and (3.22). Figure 8 displays the evolution of the distribution of the local total estimator when refining the mesh with the uniform approach (*left*) and with the adaptive one (*right*). In particular, with the adaptive approach, the interval containing all the local estimators $\{\eta_{\text{tot},T}\}_{T \in \mathcal{T}_h}$ progressively narrows with each refinement step, and the maximum value decreases significantly faster than with the uniform approach. Consequently, the distribution of the values of $\eta_{\text{tot},T}$ becomes more uniform in the adaptive case.

Finally, Table 3 shows the number of Newton iterations (3.6) required to satisfy the stopping criterion of Line 8 of the fully adaptive Algorithm 1 with $\gamma_{\text{lin}} = 0.01$. Figure 9a illustrates the evolution of the global estimators η_{tot} , η_{str} , η_{cnt} and η_{frc} as functions of the number of degrees of freedom. Additionally, the same estimators are represented as functions of the number of Newton iterations by Figure 9b and 9c for the 2nd and 10th adaptively refined meshes, respectively.



(a) H^1 -norm $\|\bar{\mathbf{u}}_h - \mathbf{u}_h\|_{1,\Omega}$ and energy norm $\|\bar{\mathbf{u}}_h - \mathbf{u}_h\|_{\text{en}}$.



(b) Global total estimator η_{tot} , lower bound $\mathcal{L}(\mathbf{u}_h)$, and upper bound $\mathcal{U}(\mathbf{u}_h)$. (c) Effectivity indices of the lower bound $I_{\text{eff,low}}$ and the upper bound $I_{\text{eff,up}}$.

Figure 7: Comparison between uniform and adaptive refinement (circles and triangles, respectively) for the Tresca test case of Section 5.1.

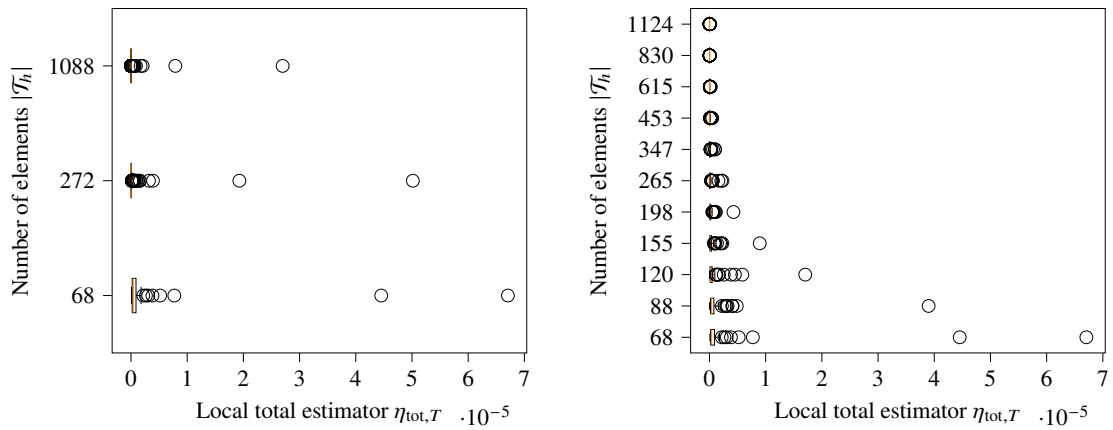


Figure 8: Distribution of the local total estimator $\eta_{\text{tot},T}$ for each spatial step with uniform (*left*) and adaptive (*right*) mesh refinement for the Tresca test case of Section 5.1.

	Initial	1 st	2 nd	3 rd	4 th	5 th	6 th	7 th	8 th	9 th	10 th
N_{lin}	3	3	3	3	4	4	4	5	5	5	5

Table 3: Number of Newton iterations at each refinement step of Algorithm 1 for the Tresca test case of Section 5.1.

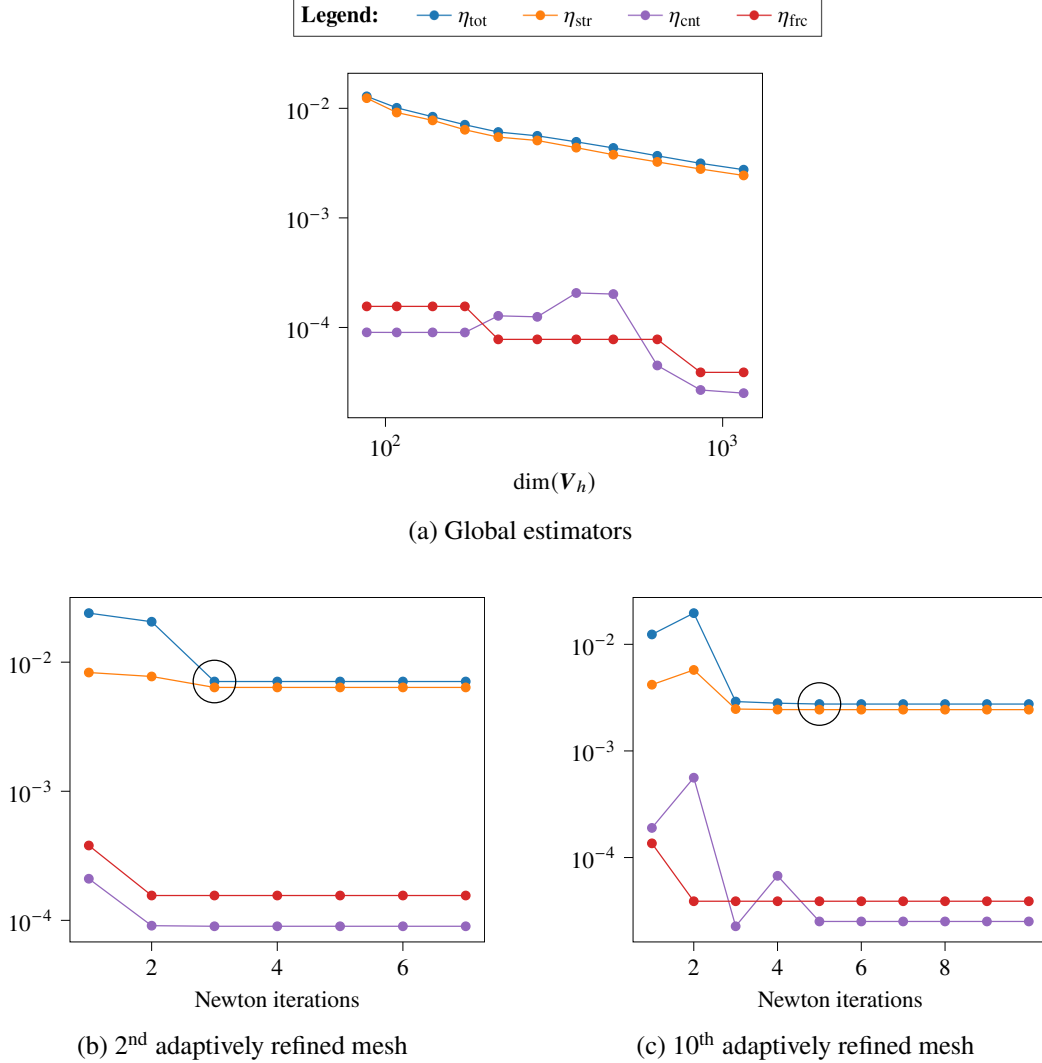
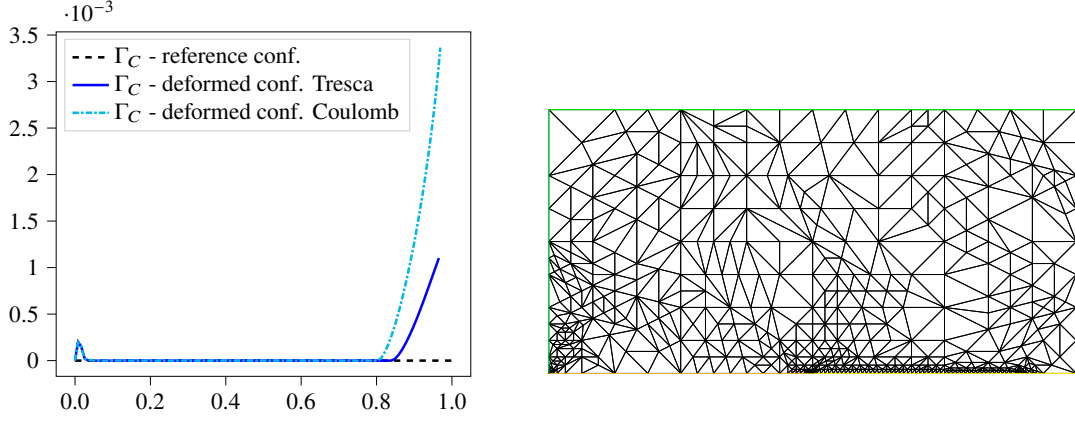


Figure 9: Evolution of the global estimators η_{tot} , η_{str} , η_{cnt} and η_{fric} using Algorithm 1 with respect to the number of degrees of freedom (*top*), and with respect to the number of Newton iterations for the 2nd and 10th adaptively refined mesh for the Tresca test case of Section 5.1. The circle indicates the Newton iteration at which the convergence criterion has been reached.

5.2 Coulomb friction

In this section, we consider again the configuration depicted in Figure 4, using the same parameters as in the previous numerical example but, this time, Coulomb friction conditions are enforced on Γ_C :



(a) Displacement on Γ_C in the deformed configuration with Tresca and Coulomb friction.

(b) Adaptively refined mesh after 10 remeshing steps.

Figure 10: Contact region and adaptively refined mesh for the Coulomb test case of Section 5.2.

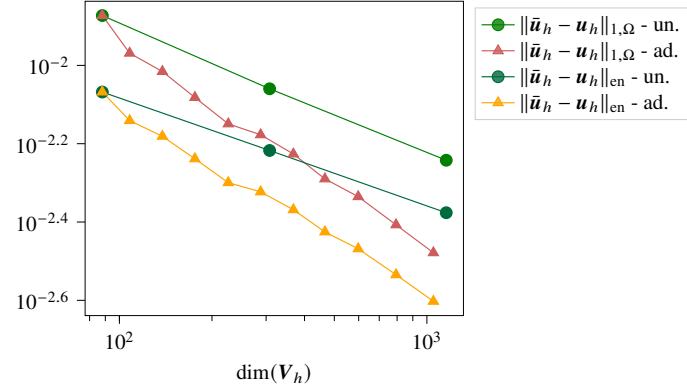
$$\left[\mathbf{P}_{1,\gamma}^t(\mathbf{u}_h) \right]_{S_h(\mathbf{u}_h)} = \begin{cases} \mathbf{0} & \text{if } P_{1,\gamma}^n(\mathbf{u}_h) > 0, \\ \mathbf{P}_{1,\gamma}^t(\mathbf{u}_h) & \text{if } |\mathbf{P}_{1,\gamma}^t(\mathbf{u}_h)| \leq -\mu_{\text{Coul}} P_{1,\gamma}^n(\mathbf{u}_h), \\ -\mu_{\text{Coul}} P_{1,\gamma}^n(\mathbf{u}_h) \frac{\mathbf{P}_{1,\gamma}^t(\mathbf{u}_h)}{|\mathbf{P}_{1,\gamma}^t(\mathbf{u}_h)|} & \text{otherwise,} \end{cases} \quad (5.4)$$

with the friction parameter $\mu_{\text{Coul}} = 0.5$. In Figure 10b, we compare the profiles of the contact boundary Γ_C in the deformed configuration (*light blue*) with the one in the reference configuration (*black*) and with the one in the deformed configuration with the Tresca boundary conditions with $s = 5 \cdot 10^{-3}$ as in the previous example (*blue*). With the selected choice of friction parameters, the opening is more significant in the Coulomb friction case. Starting from the coarse mesh of Figure 6a, we apply the same adaptive approach as in the previous example, and, after 10 remeshing steps, we obtain the mesh of Figure 10b. Once again, the refinement concentrates near the endpoints of Γ_D and on the contact boundary Γ_C , particularly along the actual contact interval $I_C \approx (0.035, 0.802)$.

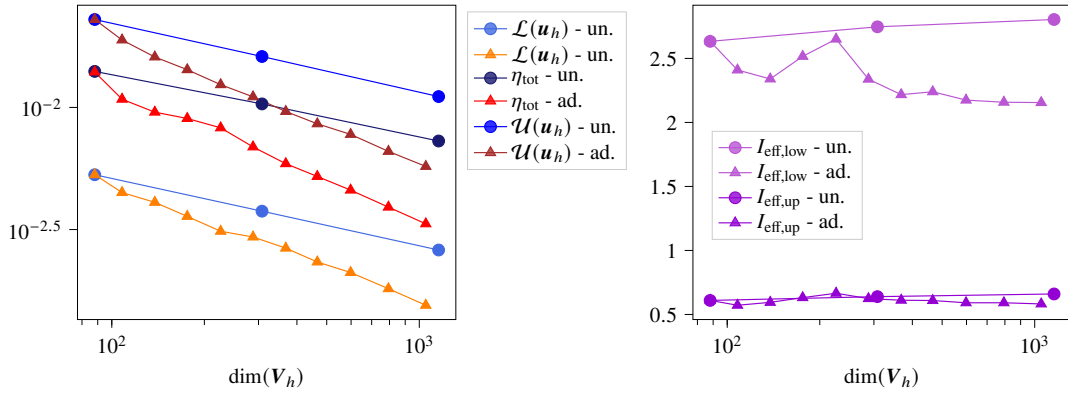
We then compare the results obtained with uniform and adaptive approaches: Figure 11 showcases the convergence of the H^1 -norm $\|\bar{\mathbf{u}} - \mathbf{u}_h\|_{1,\Omega}$ and energy norm $\|\bar{\mathbf{u}} - \mathbf{u}_h\|_{\text{en}}$, along with the comparison of the global total estimator η_{tot} with the bounds $\mathcal{L}(\mathbf{u}_h)$ and $\mathcal{U}(\mathbf{u}_h)$ defined by (5.1) and (5.2), as well as the corresponding effectivity indices (5.3). Additionally, Figure 12 represents the distribution of the total local estimators $\{\eta_{\text{tot},T}\}_{T \in \mathcal{T}_h}$. Notably, the results mirror those observed in the previous example. Specifically, in this case the asymptotic rates of convergence of H^1 -norm and energy norm are approximately 0.317 and 0.277 for the uniform case, 0.496 and 0.513 for the adaptive one.

5.3 A test case from literature

We conclude this section by considering the setting of the numerical test investigated in [21]. We consider an elastic object represented by the square domain $\Omega = (0, 1)^2$, with Young modulus $E = 10^6$ and Poisson ratio $\nu = 0.3$. This domain is subject to a vertical force $\mathbf{f} = (0, -76518)$, it is clamped on $\Gamma_D = \{0\} \times (0, 1)$, and no force is applied on $\Gamma_N = (0, 1) \times \{0\} \cap \{1\}$. On the contact



(a) H^1 -norm $\|\bar{\mathbf{u}} - \mathbf{u}_h\|_{1,\Omega}$ and energy norm $\|\bar{\mathbf{u}} - \mathbf{u}_h\|_{\text{en}}$.



(b) Global total estimator η_{tot} , lower bound $\mathcal{L}(\mathbf{u}_h)$, and upper bound $\mathcal{U}(\mathbf{u}_h)$. (c) Effectivity indices of the lower bound $I_{\text{eff,low}}$ and the upper bound $I_{\text{eff,up}}$.

Figure 11: Comparison between uniform and adaptive refinement (circles and triangles, respectively) for the Coulomb test case of Section 5.2.

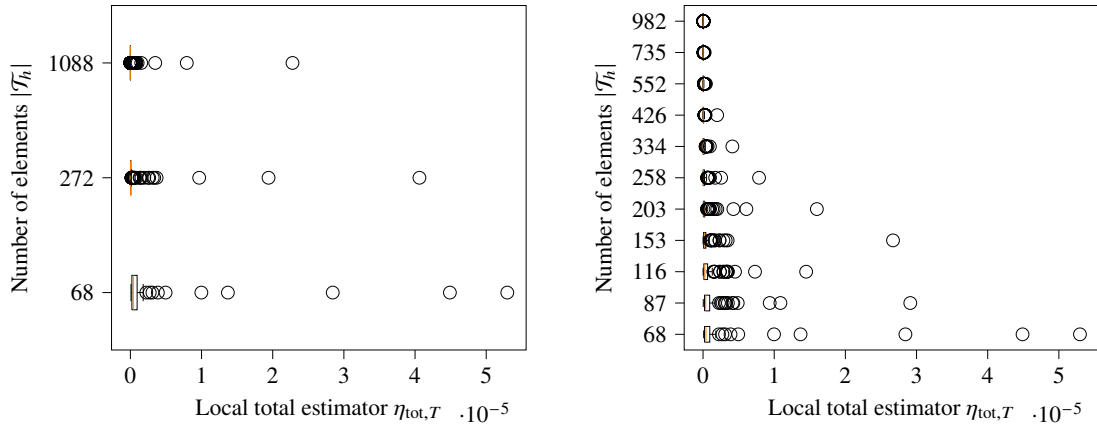


Figure 12: Distribution of the local total estimator $\eta_{\text{tot},T}$ for each spatial step with uniform (left) and adaptive (right) refinement approach for the Coulomb test case of Section 5.2.

boundary part $\Gamma_C = \{1\} \times (0, 1)$, Coulomb boundary conditions (5.4) are enforced with the friction

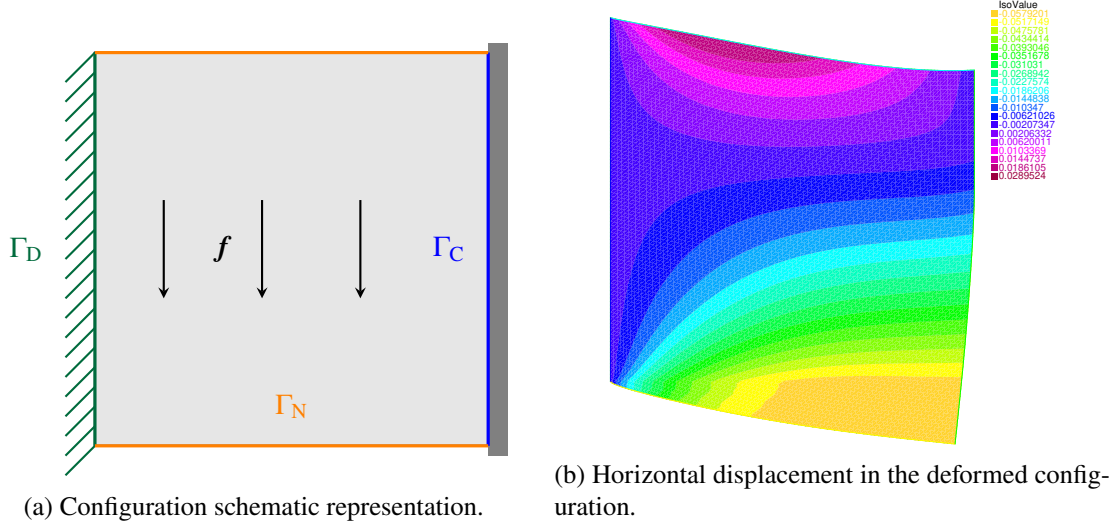


Figure 13: Square domain for the test case of Section 5.3 (configuration from [21]) with representation of internal forces and division of the domain’s boundary. In particular, homogeneous Neumann conditions are enforced on Γ_N . The portion of the boundary Γ_D is fixed, while contact is possible on Γ_C .

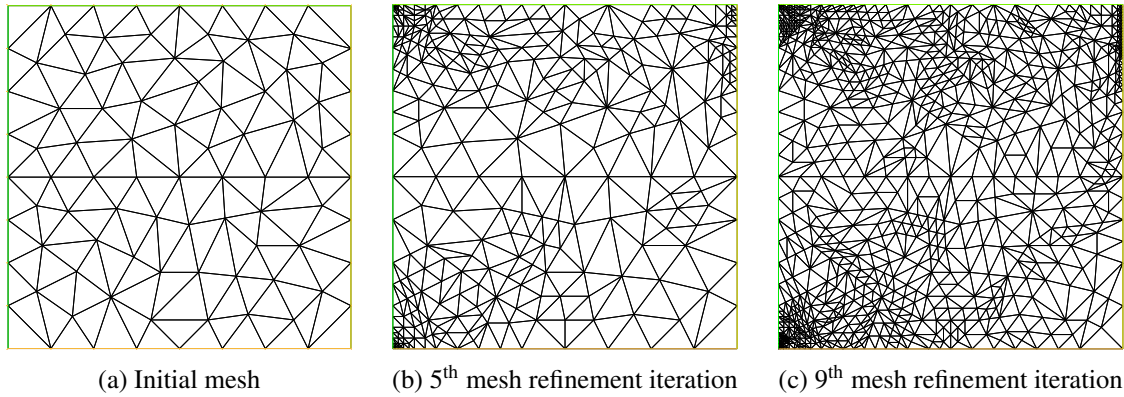
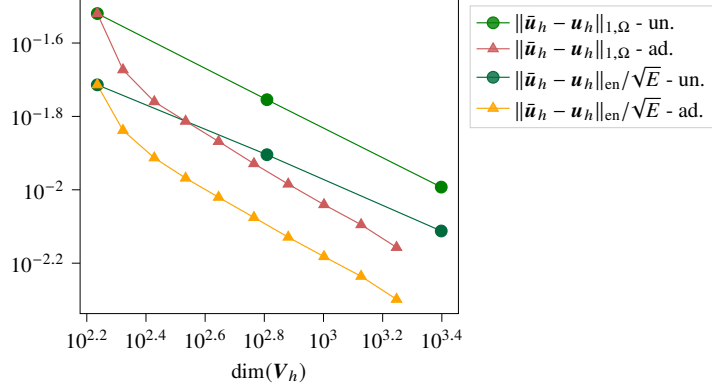


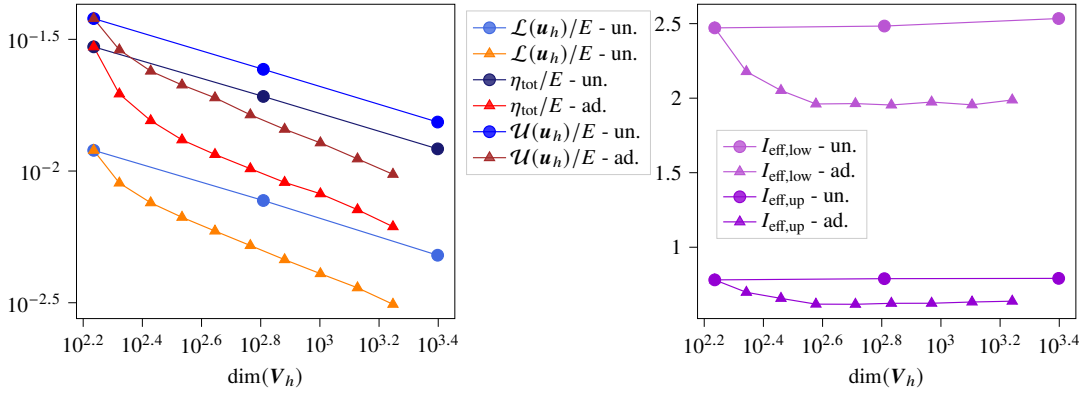
Figure 14: Initial mesh and adaptively refined mesh after 5, and 9 remeshing steps, respectively, for the test case of Section 5.3.

parameter $\mu_{\text{Coul}} = 0.2$. Additionally, the Nitsche parameter is set to $\gamma_0 = E$ as in [7]. Figure 13 shows this setting (*left*) together with the horizontal displacement in the deformed configuration (*right*). For this configuration, as before, the reference solution $\bar{\mathbf{u}}_h$ is computed solving the discrete problem (2.11) using \mathcal{P}^2 Lagrange finite elements on a fine mesh with mesh size $h \approx 8.34 \cdot 10^{-3}$, while the approximate solution \mathbf{u}_h is obtained using \mathcal{P}^1 Lagrange finite elements and the adaptive algorithm described in Subsection 3.2. Also in this case, on the contact boundary Γ_C we observe both slip and separation.

We start from the mesh depicted in Figure 14a and refine at each spatial iteration at least 6.2% of the elements. After 5 and 9 steps, respectively, we obtain the meshes of Figures 14b and 14c. Notice that the refinement is concentrated around the endpoints of Γ_D and the actual contact interval $I_C \subset \Gamma_C$. Additionally, Figure 15a shows the evolution of the H^1 -norm $\|\bar{\mathbf{u}} - \mathbf{u}_h\|_{1,\Omega}$ and energy norm $\|\bar{\mathbf{u}} - \mathbf{u}_h\|_{\text{en}}$, which asymptotic rates are approximately 0.404 and 0.353 in the uniform case, and 0.516 and 0.522 in the adaptive one. The total estimators η_{tot} , the lower bound $\mathcal{L}(\mathbf{u}_h)$, and



(a) H^1 -norm $\|\bar{\mathbf{u}} - \mathbf{u}_h\|_{1,\Omega}$ and energy norm $\|\bar{\mathbf{u}} - \mathbf{u}_h\|_{\text{en}}/\sqrt{E}$.



(b) Global total estimator η_{tot} , lower bound $\mathcal{L}(\mathbf{u}_h)$, and upper bound $\mathcal{U}(\mathbf{u}_h)$, divided by E .

(c) Effectivity indices of the lower bound $I_{\text{eff,low}}$ and the upper bound $I_{\text{eff,up}}$.

Figure 15: Comparison between uniform and adaptive refinement (circles and triangles, respectively) for the test case of Section 5.3.

the upper bound $\mathcal{U}(\mathbf{u}_h)$ are displayed in Figure 15b, and the corresponding effectivity indices in Figure 15c. Results similar to the ones of Figure 8 can be obtained for the distribution of the local total estimators.

6 Efficiency of the estimators

In this section, we prove the efficiency of the estimators introduced in Section 3.2 using the stress reconstruction σ_h described in Section 4. As before, we will use the notation $a \lesssim b$, $a, b \in \mathbb{R}$ when $a \leq Cb$ where $C > 0$ is a constant independent of the mesh size h and of the Nitsche parameter γ_0 . We start presenting the results of local and global efficiency, and then we explain the main idea of their proofs.

To show local efficiency, we work on local patches around elements of the mesh [26]. For any mesh element $T \in \mathcal{T}_h$, we introduce the patch $\tilde{\omega}_T$ defined as the union of all elements sharing at least one vertex with T and denote by $\mathcal{T}_{\tilde{\omega}_T}$ the corresponding set of elements. Then, we define the

local residual operator $\mathcal{R}_{\mathcal{T}_T} : \mathbf{V}_h \rightarrow (\mathbf{H}_D^1(\tilde{\omega}_T))^*$ by: For all $\mathbf{w}_h \in \mathbf{V}_h$ and all $\mathbf{v} \in \mathbf{H}_D^1(\tilde{\omega}_T)$.

$$\begin{aligned} \langle \mathcal{R}_{\mathcal{T}_T}(\mathbf{w}_h), \mathbf{v} \rangle_{\tilde{\omega}_T} &:= (\mathbf{f}, \mathbf{v})_{\tilde{\omega}_T} + (\mathbf{g}_N, \mathbf{v})_{\partial\tilde{\omega}_T \cap \Gamma_N} - (\boldsymbol{\sigma}(\mathbf{w}_h), \boldsymbol{\varepsilon}(\mathbf{v}))_{\tilde{\omega}_T} \\ &\quad + \left(\left[P_{1,\gamma}^n(\mathbf{w}_h) \right]_{\mathbb{R}^-}, \mathbf{v}^n \right)_{\partial\tilde{\omega}_T \cap \Gamma_C} + \left(\left[\mathbf{P}_{1,\gamma}^t(\mathbf{w}_h) \right]_{S_h(\mathbf{w}_h)}, \mathbf{v}_h^t \right)_{\partial\tilde{\omega}_T \cap \Gamma_C}. \end{aligned}$$

Here, the space $\mathbf{H}_D^1(\tilde{\omega}_T)$ is the natural restriction of $\mathbf{H}_D^1(\Omega)$ to the patch $\tilde{\omega}_T$, i.e.,

$$\mathbf{H}_D^1(\tilde{\omega}_T) := \{ \mathbf{v} \in \mathbf{H}^1(\tilde{\omega}_T) : \mathbf{v} = \mathbf{0} \text{ on } \partial\tilde{\omega}_T \cap \Gamma_D \text{ and on } \partial\tilde{\omega}_T \cap \Omega \}.$$

Finally, letting

$$\|\mathbf{v}\|_{\tilde{\omega}_T} := \left(\|\nabla \mathbf{v}\|_{\tilde{\omega}_T}^2 + |\mathbf{v}|_{C,\tilde{\omega}_T}^2 \right)^{1/2} = \left(\|\nabla \mathbf{v}\|_{\tilde{\omega}_T}^2 + \sum_{F \in \mathcal{F}_{\mathcal{T}_T}^C} \frac{1}{h_F} \|\mathbf{v}\|_F^2 \right)^{1/2},$$

with $\mathcal{F}_{\mathcal{T}_T}^C$ denoting the (possibly empty) set of faces of \mathcal{T}_T that lie on Γ_C , we get, for a function $\mathbf{w}_h \in \mathbf{V}_h$, the local residual norm

$$\|\mathcal{R}_{\mathcal{T}_T}(\mathbf{w}_h)\|_{*,\tilde{\omega}_T} = \sup_{\mathbf{v} \in \mathbf{H}_D^1(\tilde{\omega}_T), \|\mathbf{v}\|_{\tilde{\omega}_T}=1} \langle \mathcal{R}_{\mathcal{T}_T}(\mathbf{w}_h), \mathbf{v} \rangle_{\tilde{\omega}_T}. \quad (6.1)$$

Theorem 15 (Local efficiency). Assume $d = 2$. Let $\mathbf{u}_h^k \in \mathbf{V}_h$ be the approximate solution obtained with Algorithm 1 replacing Line 8 with the local stopping criterion (3.15), and let $\boldsymbol{\sigma}_h^k$ be the stress field resulting from Construction 12. Then, for every element $T \in \mathcal{T}_h$, it holds

$$\eta_{\text{str},T}^k \lesssim \|\mathcal{R}_{\mathcal{T}_T}(\mathbf{u}_h^k)\|_{*,\tilde{\omega}_T} + \eta_{\text{osc},\mathcal{T}_T}^k + \eta_{\text{Neu},\mathcal{T}_T}^k + \eta_{\text{cnt},\mathcal{T}_T}^k + \eta_{\text{frc},\mathcal{T}_T}^k, \quad (6.2)$$

and, as a consequence,

$$\begin{aligned} \eta_{\text{osc},T}^k + \eta_{\text{str},T}^k + \eta_{\text{Neu},T}^k + \eta_{\text{cnt},T}^k + \eta_{\text{frc},T}^k + \eta_{\text{lin},T}^k \\ \lesssim \|\mathcal{R}_{\mathcal{T}_T}(\mathbf{u}_h^k)\|_{*,\tilde{\omega}_T} + \eta_{\text{osc},\mathcal{T}_T}^k + \eta_{\text{Neu},\mathcal{T}_T}^k + \eta_{\text{cnt},\mathcal{T}_T}^k + \eta_{\text{frc},\mathcal{T}_T}^k, \end{aligned} \quad (6.3)$$

where

$$\eta_{\bullet,\mathcal{T}_T}^k := \left[\sum_{T' \in \mathcal{T}_T} \left(\eta_{\bullet,T'}^k \right)^2 \right]^{1/2} \quad \text{with } \bullet \in \{\text{osc}, \text{Neu}, \text{cnt}\}. \quad (6.4)$$

Theorem 16 (Global efficiency). Assume $d = 2$. Let $\mathbf{u}_h^k \in \mathbf{V}_h$ the approximate solution obtained with Algorithm 1, and let $\boldsymbol{\sigma}_h^k$ be the stress field resulting from Construction 12. Then, it holds

$$\eta_{\text{str}}^k \lesssim \|\mathcal{R}(\mathbf{u}_h^k)\|_* + \eta_{\text{osc}}^k + \eta_{\text{Neu}}^k + \eta_{\text{cnt}}^k + \eta_{\text{frc}}^k, \quad (6.5)$$

and, as a consequence,

$$\eta_{\text{osc}}^k + \eta_{\text{str}}^k + \eta_{\text{Neu}}^k + \eta_{\text{cnt}}^k + \eta_{\text{frc}}^k + \eta_{\text{lin}}^k \lesssim \|\mathcal{R}(\mathbf{u}_h^k)\|_* + \eta_{\text{osc}}^k + \eta_{\text{Neu}}^k + \eta_{\text{cnt}}^k + \eta_{\text{frc}}^k. \quad (6.6)$$

6.1 Proof of the local efficiency

We illustrate the main steps of the proof of Theorem 15. To this end, we will need the notion of *bubble function* of an element $T \in \mathcal{T}_h$ and of a face $F \in \mathcal{F}_h$ defined starting from the hat function ψ_a :

$$\psi_T := \alpha_T \prod_{a \in \mathcal{V}_T} \psi_a \in \mathcal{P}^{d+1}(T), \quad \psi_F := \alpha_F \prod_{a \in \mathcal{V}_F} \psi_a \in \mathcal{P}^d(\omega_F),$$

where the constants α_T and α_F are determined by the conditions $\max_{\mathbf{x} \in T} \psi_T(\mathbf{x}) = 1$ and $\max_{\mathbf{x} \in F} \psi_F(\mathbf{x}) = 1$. Additionally, we will need the following four properties of these bubble functions (see [27, Section 3.1]):

$$\|\mathbf{v}\|_T^2 \lesssim (\psi_T \mathbf{v}, \mathbf{v})_T \leq \|\mathbf{v}\|_T^2, \quad (6.7a)$$

$$\|\psi_T \mathbf{v}\|_{1,T} \lesssim \frac{1}{h_T} \|\mathbf{v}\|_T, \quad (6.7b)$$

$$\|\boldsymbol{\varphi}\|_F^2 \lesssim (\psi_F \boldsymbol{\varphi}, \boldsymbol{\varphi})_F \leq \|\boldsymbol{\varphi}\|_F^2, \quad (6.7c)$$

$$\|\psi_F \boldsymbol{\varphi}\|_{\omega_F} + h_F \|\psi_F \boldsymbol{\varphi}\|_{1,\omega_F} \lesssim h_F^{1/2} \|\boldsymbol{\varphi}\|_F, \quad (6.7d)$$

where $T \in \mathcal{T}_h$, $F \in \mathcal{F}_h$, \mathbf{v} , and $\boldsymbol{\varphi}$ are d -valued polynomials of degree at most r defined on T and ω_F , respectively. The hidden constants depend only on the polynomial degree r and on the shape regularity parameter of the mesh.

Remark 17 (Extension of (6.7a) and (6.7c)). Following the path of [15], it is possible to show that for any $S \subseteq \mathcal{T}_h$ and any $\mathbf{v} \in \mathcal{P}^r(S)$

$$\left(\sum_{T \in S} h_T^2 \|\mathbf{v}\|_T^2 \right)^{1/2} \lesssim \sup_{\substack{\mathbf{w} \in \mathcal{P}^r(S), \\ \|\mathbf{w}\|_{\omega_S} = 1}} \sum_{T \in S} (\mathbf{v}, h_T \psi_T \mathbf{w})_T. \quad (6.8)$$

where $\omega_S := \bigcup_{T \in S} T$ and $\|\mathbf{w}\|_{\omega_S} := (\sum_{T \in S} \|\mathbf{w}\|_T^2)^{1/2}$. In a similar way, for any $\mathcal{E} \subseteq \mathcal{F}_h$ and any $\boldsymbol{\varphi} \in \mathcal{P}^r(\mathcal{E})$

$$\left(\sum_{F \in \mathcal{E}} h_F \|\boldsymbol{\varphi}\|_F^2 \right)^{1/2} \lesssim \sup_{\substack{\boldsymbol{\phi} \in \mathcal{P}^r(\mathcal{E}), \\ \|\boldsymbol{\phi}\|_{\mathcal{E}} = 1}} \sum_{F \in \mathcal{E}} (\boldsymbol{\varphi}, h_F^{1/2} \psi_F \boldsymbol{\phi})_F \quad (6.9)$$

where $\|\boldsymbol{\phi}\|_{\mathcal{E}} := (\sum_{F \in \mathcal{E}} \|\boldsymbol{\phi}\|_F^2)^{1/2}$.

Following [26], for any element $T \in \mathcal{T}_h$ we introduce a local *residual based estimator* defined on the local patch $\tilde{\omega}_T$:

$$\begin{aligned} \eta_{\sharp,T}^k &:= \left(\sum_{T' \in \mathcal{T}_T} h_{T'}^2 \|\mathbf{div} \boldsymbol{\sigma}(\mathbf{u}_h^k) + \boldsymbol{\Pi}_{T'}^p \mathbf{f}\|_{T'}^2 \right)^{1/2} + \left(\sum_{F \in \mathcal{F}_{\mathcal{T}_T}^i} h_F \|\llbracket \boldsymbol{\sigma}(\mathbf{u}_h^k) \mathbf{n}_F \rrbracket\|_F^2 \right)^{1/2} \\ &\quad + \left(\sum_{F \in \mathcal{F}_{\mathcal{T}_T}^N} h_F \|\boldsymbol{\sigma}(\mathbf{u}_h^k) \mathbf{n} - \boldsymbol{\Pi}_F^{p+1} \mathbf{g}_N\|_F^2 \right)^{1/2} \\ &\quad + \left(\sum_{F \in \mathcal{F}_{\mathcal{T}_T}^C} h_F \|\boldsymbol{\sigma}^n(\mathbf{u}_h^k) - \boldsymbol{\Pi}_F^{p+1} [\mathbf{P}_{1,\gamma}^n(\mathbf{u}_h^k)]_{\mathbb{R}^-}\|_F^2 \right)^{1/2} \\ &\quad + \left(\sum_{F \in \mathcal{F}_{\mathcal{T}_T}^C} h_F \|\boldsymbol{\sigma}^t(\mathbf{u}_h^k) - \boldsymbol{\Pi}_F^{p+1} [\mathbf{P}_{1,\gamma}^t(\mathbf{u}_h^k)]_{S_h(\mathbf{u}_h^k)}\|_F^2 \right)^{1/2}. \end{aligned} \quad (6.10)$$

Lemma 18 (Control of the residual-based estimator $\eta_{\sharp,T}^k$). Let $\mathbf{u}_h^k \in \mathbf{V}_h$, let $\boldsymbol{\sigma}_h^k$ be the equilibrated stress defined by Construction 12, and let $\eta_{\sharp,T}^k$ be the local residual-based estimator defined by (6.10). Then, for any element $T \in \mathcal{T}_h$,

$$\eta_{\sharp,T}^k \lesssim \|\mathcal{R}_{\mathcal{T}_T}(\mathbf{u}_h^k)\|_{*,\tilde{\omega}_T} + \eta_{\text{osc},\mathcal{T}_T}^k + \eta_{\text{Neu},\mathcal{T}_T}^k + \eta_{\text{cnt},\mathcal{T}_T}^k + \eta_{\text{frc},\mathcal{T}_T}^k. \quad (6.11)$$

Proof of Lemma 18. Let us fix an element $T \in \mathcal{T}_h$. We analyze each term on the right-hand side of (6.10) separately. For simplicity, we denote them with $\mathcal{J}_1, \mathcal{J}_2, \mathcal{J}_3, \mathcal{J}_4$, and \mathcal{J}_5 , respectively. The key idea is to use the above-mentioned inequalities involving the bubble functions: (6.8) with $\mathcal{S} = \mathcal{T}_T$ for \mathcal{J}_1 and (6.9) with $\mathcal{E} = \mathcal{F}_{\mathcal{T}_T}^i, \mathcal{F}_{\mathcal{T}_T}^N, \mathcal{F}_{\mathcal{T}_T}^C$ for $\mathcal{J}_2, \mathcal{J}_3, \mathcal{J}_4$, and \mathcal{J}_5 .

Since $(\nabla \cdot \boldsymbol{\sigma}(\mathbf{u}_h^k))|_{T'} + \mathbf{\Pi}_{T'}^p \mathbf{f}|_{T'} \in \mathcal{P}^p(T')$ for every $T' \in \mathcal{T}_T$, applying (6.8) we get

$$\mathcal{J}_1 \lesssim \sup_{\substack{\mathbf{w} \in \mathcal{P}^p(\mathcal{T}_T), \\ \|\mathbf{w}\|_{\tilde{\omega}_T} = 1}} \sum_{T' \in \mathcal{T}_T} (\mathbf{div} \boldsymbol{\sigma}(\mathbf{u}_h^k) + \mathbf{\Pi}_{T'}^p \mathbf{f}, h_{T'} \psi_{T'} \mathbf{w})_{T'}. \quad (6.12)$$

Notice that here we simply write $\|\mathbf{w}\|_{\tilde{\omega}_T}$ instead of $\|\mathbf{w}\|_{\omega_{\mathcal{T}_T}}$. Fix $\mathbf{w} \in \mathcal{P}^p(\mathcal{T}_T)$ with $\|\mathbf{w}\|_{\tilde{\omega}_T} = 1$, and define $\lambda|_{T'} := h_{T'} \psi_{T'} \mathbf{w}|_{T'}$ for every $T' \in \mathcal{T}_T$. Notice that $\lambda \in \mathcal{P}^{p+d+1}(\mathcal{T}_T) \cap \mathbf{H}_D^1(\tilde{\omega}_T)$. Then, using an integration by parts on each element $T' \in \mathcal{T}_T$, the definition of the residual, and the Cauchy–Schwarz inequality we obtain

$$\begin{aligned} & \sum_{T' \in \mathcal{T}_T} (\mathbf{div} \boldsymbol{\sigma}(\mathbf{u}_h^k) + \mathbf{\Pi}_{T'}^p \mathbf{f}, h_{T'} \psi_{T'} \mathbf{w})_{T'} \\ & \lesssim \|\mathcal{R}_{\mathcal{T}_T}(\mathbf{u}_h^k)\|_{*,\tilde{\omega}_T} \|\lambda\|_{\tilde{\omega}_T} + \left(\sum_{T' \in \mathcal{T}_T} h_{T'}^2 \|\mathbf{f} - \mathbf{\Pi}_{T'}^{p-1} \mathbf{f}\|_{T'}^2 \right)^{1/2} \left(\sum_{T' \in \mathcal{T}_T} \|\psi_{T'} \mathbf{w}\|_{T'}^2 \right)^{1/2}. \end{aligned} \quad (6.13)$$

Here, we have also used the fact that $\|\mathbf{f} - \mathbf{\Pi}_{T'}^p \mathbf{f}\|_{T'} \leq 2\|\mathbf{f} - \mathbf{\Pi}_{T'}^{p-1} \mathbf{f}\|_{T'}$ for $p > 0$. By the definition of λ , properties (6.7a) and (6.7b), along with the fact that $\|\mathbf{w}\|_{\tilde{\omega}_T} = 1$, it is possible to show that

$$\|\lambda\|_{\tilde{\omega}_T} \lesssim 1 \quad \text{and} \quad \left(\sum_{T' \in \mathcal{T}_T} \|\psi_{T'} \mathbf{w}\|_{T'}^2 \right)^{1/2} \lesssim 1,$$

and, combining the above results with (4.4a), we conclude

$$\mathcal{J}_1 \lesssim \|\mathcal{R}_{\mathcal{T}_T}(\mathbf{u}_h^k)\|_{*,\tilde{\omega}_T} + \eta_{\text{osc},\mathcal{T}_T}^k. \quad (6.14)$$

Now, we analyze for instance the term \mathcal{J}_5 : $\mathcal{J}_2, \mathcal{J}_3$ and \mathcal{J}_4 can be treated in a similar way. Using the fact that $\boldsymbol{\sigma}^t(\mathbf{u}_h^k) - \mathbf{\Pi}_F^{p+1} \left[\mathbf{P}_{1,\gamma}^t(\mathbf{u}_h^k) \right]_{S_h(\mathbf{u}_h^k)} \in \mathcal{P}^{p+1}(F)$ for every $F \in \mathcal{F}_{\mathcal{T}_T}^C$ along with (6.9), we have

$$\mathcal{J}_4 \lesssim \sup_{\substack{\boldsymbol{\phi} \in \mathcal{P}^{p+1}(\mathcal{F}_{\mathcal{T}_T}^C), \\ \|\boldsymbol{\phi}\|_{\mathcal{F}_{\mathcal{T}_T}^C} = 1}} \sum_{F \in \mathcal{F}_{\mathcal{T}_T}^C} \left(\boldsymbol{\sigma}^t(\mathbf{u}_h^k) - \mathbf{\Pi}_F^{p+1} \left[\mathbf{P}_{1,\gamma}^t(\mathbf{u}_h^k) \right]_{S_h(\mathbf{u}_h^k)}, h_F^{1/2} \psi_F \boldsymbol{\phi} \right)_F. \quad (6.15)$$

Fix $\boldsymbol{\phi} \in \mathcal{P}^{p+1}(\mathcal{F}_{\mathcal{T}_T}^C)$ with $\|\boldsymbol{\phi}\|_{\mathcal{F}_{\mathcal{T}_T}^C} = 1$, and define $\lambda \in \mathcal{P}^{p+d+1}(\mathcal{T}_T) \cap \mathbf{H}_D^1(\tilde{\omega}_T)$ satisfying $\lambda|_F = h_F^{1/2} \psi_F \boldsymbol{\phi}|_F$ for every $F \in \mathcal{F}_{\mathcal{T}_T}^C$ and vanishing outside of $\bigcup_{F \in \mathcal{F}_{\mathcal{T}_T}^C} \omega_F$. Then, using the Cauchy–

Schwarz inequality together with (4.4a) and (4.4d) we get

$$\begin{aligned}
& \sum_{F \in \mathcal{F}_T^c} \left(\boldsymbol{\sigma}^t(\mathbf{u}_h^k) - \boldsymbol{\Pi}_F^{p+1} \left[\mathbf{P}_{1,\gamma}^t(\mathbf{u}_h^k) \right]_{S_h(\mathbf{u}_h^k)}, h_F^{1/2} \boldsymbol{\psi}_F \boldsymbol{\phi} \right)_F \\
&= - \langle \mathcal{R}_{\mathcal{T}_T}(\mathbf{u}_h^k), \boldsymbol{\lambda} \rangle_{\tilde{\omega}_T} + \sum_{T' \in \mathcal{T}_T} (\nabla \cdot \boldsymbol{\sigma}(\mathbf{u}_h^k) + \mathbf{f}, \boldsymbol{\lambda})_{T'} \\
&+ \sum_{F \in \mathcal{F}_T^c} \left(\left[\mathbf{P}_{1,\gamma}^t(\mathbf{u}_h^k) \right]_{S_h(\mathbf{u}_h^k)} - \boldsymbol{\Pi}_F^{p+1} \left[\mathbf{P}_{1,\gamma}^t(\mathbf{u}_h^k) \right]_{S_h(\mathbf{u}_h^k)}, \boldsymbol{\lambda} \right)_F \quad (6.16) \\
&\lesssim \| \mathcal{R}_{\mathcal{T}_T}(\mathbf{u}_h^k) \|_{*, \tilde{\omega}_T} \| \boldsymbol{\lambda} \|_{\tilde{\omega}_T} + (\mathcal{J}_1 + \eta_{\text{osc}, \mathcal{T}_T}^k) \left(\sum_{T' \in \mathcal{T}_T} \frac{1}{h_{T'}^2} \| \boldsymbol{\lambda} \|_{T'}^2 \right)^{1/2} \\
&+ \eta_{\text{irc}, \mathcal{T}_T}^k \left(\sum_{F \in \mathcal{F}_T^c} \frac{1}{h_F} \| \boldsymbol{\lambda} \|_F^2 \right)^{1/2}.
\end{aligned}$$

Exploiting the properties (6.7c) and (6.7d), it is possible to show that

$$\| \boldsymbol{\lambda} \|_{\tilde{\omega}_T} \lesssim 1, \quad \left(\sum_{T' \in \mathcal{T}_T} \frac{1}{h_{T'}^2} \| \boldsymbol{\lambda} \|_{T'}^2 \right)^{1/2} \lesssim 1 \quad \text{and} \quad \left(\sum_{F \in \mathcal{F}_T^c} \frac{1}{h_F} \| \boldsymbol{\lambda} \|_F^2 \right)^{1/2} \lesssim 1,$$

and, combining (6.15), (6.16), and (6.14), we conclude that

$$\mathcal{J}_4 \lesssim \| \mathcal{R}_{\mathcal{T}_T}(\mathbf{u}_h^k) \|_{*, \tilde{\omega}_T} + \eta_{\text{osc}, \mathcal{T}_T}^k + \eta_{\text{irc}, \mathcal{T}_T}^k.$$

Proceeding in a similar way, it is possible to obtain the following bounds:

$$\begin{aligned}
\mathcal{J}_2 &\lesssim \| \mathcal{R}_{\mathcal{T}_T}(\mathbf{u}_h^k) \|_{*, \tilde{\omega}_T} + \eta_{\text{osc}, \mathcal{T}_T}^k, \\
\mathcal{J}_3 &\lesssim \| \mathcal{R}_{\mathcal{T}_T}(\mathbf{u}_h^k) \|_{*, \tilde{\omega}_T} + \eta_{\text{osc}, \mathcal{T}_T}^k + \eta_{\text{Neu}, \mathcal{T}_T}^k, \\
\mathcal{J}_4 &\lesssim \| \mathcal{R}_{\mathcal{T}_T}(\mathbf{u}_h^k) \|_{*, \tilde{\omega}_T} + \eta_{\text{osc}, \mathcal{T}_T}^k + \eta_{\text{cnt}, \mathcal{T}_T}^k.
\end{aligned}$$

Combining all the results obtained so far gives (6.11). \square

Lemma 19 (Control of the local stress estimator). *Assume $d = 2$. Let $\mathbf{u}_h^k \in \mathbf{V}_h$, let $\boldsymbol{\sigma}_h^k$ be the equilibrated stress defined by Construction 12, and let $\eta_{\sharp, T}^k$ be the local residual-based estimator defined by (6.10). Then, for every element $T \in \mathcal{T}_h$,*

$$\eta_{\text{str}, T}^k \lesssim \eta_{\sharp, T}^k. \quad (6.17)$$

Proof. Following the path of [4], for any element $T \in \mathcal{T}_h$ we introduce the following local nonconforming space [2]:

$$\mathbf{M}_T := \begin{cases} \{ \mathbf{m} \in \mathcal{P}^{p+2}(T) : \mathbf{m}|_F \in \mathcal{P}^{p+1}(F) \text{ for any } F \in \mathcal{F}_T \} & \text{if } p \text{ is even,} \\ \{ \mathbf{m} \in \mathcal{P}^{p+2}(T) : \mathbf{m}|_F \in \mathcal{P}^p(F) \oplus \tilde{\mathcal{P}}^{p+2}(F) \text{ for any } F \in \mathcal{F}_T \} & \text{if } p \text{ is odd,} \end{cases}$$

where $\tilde{\mathcal{P}}^{p+2}(F)$ is the $L^2(F)$ -orthogonal complement of $\mathcal{P}^{p+1}(F)$ in $\mathcal{P}^{p+2}(F)$. Then, for any vertex \mathbf{a} , on the patch $\omega_{\mathbf{a}}$ we define the spaces

$$\begin{aligned}
\mathbf{M}_h(\omega_{\mathbf{a}}) &:= \{ \mathbf{m}_h \in \mathbf{L}^2(\omega_{\mathbf{a}}) : \mathbf{m}_h|_T \in \mathbf{M}_T \text{ for any } T \in \mathcal{T}_{\mathbf{a}}, \\
&([\mathbf{m}_h], \mathbf{v}_h)_F = 0 \text{ for any } \mathbf{v}_h \in \mathcal{P}^p(F) \text{ and for any } F \in \mathcal{F}_{\mathbf{a}} \setminus \mathcal{F}_h^b \},
\end{aligned}$$

and

$$\mathbf{M}_h^a := \begin{cases} \{\mathbf{m}_h \in \mathbf{M}_h(\omega_a) : (\mathbf{m}_h, \mathbf{z})_{\omega_a} = 0 \text{ for any } \mathbf{z} \in \mathbf{R}\mathbf{M}^2\} & \text{if } \mathbf{a} \in \mathcal{V}_h^i \text{ or } \mathbf{a} \in \mathcal{V}_h^b \setminus \mathcal{V}_h^D, \\ \{\mathbf{m}_h \in \mathbf{M}_h(\omega_a) : (\mathbf{m}_h, \mathbf{v})_F = 0 \\ \text{for any } \mathbf{v} \in \mathcal{P}^p(F) \text{ and for any } F \in \mathcal{F}_a \cap \mathcal{F}_h^D\} & \text{if } \mathbf{a} \in \mathcal{V}_h^D. \end{cases}$$

Now, fix $T \in \mathcal{T}_h$. Combining the definition of the local stress estimator (3.10b), of $\sigma_{h,\text{dis}}^k$ given by Construction 12, of the hat function ψ_a with the triangle inequality, we directly get

$$\eta_{\text{str},T}^k = \left\| \sigma_{h,\text{dis}}^k - \sigma(\mathbf{u}_h^k) \right\|_T \leq \sum_{\mathbf{a} \in \mathcal{V}_T} \left\| \sigma_{h,\text{dis}}^{\mathbf{a},k} - \psi_a \sigma(\mathbf{u}_h^k) \right\|_{\omega_a}. \quad (6.18)$$

Adapting the argument of [4, Section 4.4] to our problem with Neumann and frictional contact boundary conditions, it is possible to show that, for any $\mathbf{a} \in \mathcal{V}_h$,

$$\left\| \sigma_{h,\text{dis}}^{\mathbf{a},k} - \psi_a \sigma(\mathbf{u}_h^k) \right\|_{\omega_a} \lesssim \sup_{\substack{\mathbf{m}_h \in \mathbf{M}_h^{\mathbf{a}}, \\ \|\nabla_h \mathbf{m}_h\|_{\omega_a} = 1}} (\sigma_{h,\text{dis}}^{\mathbf{a},k} - \psi_a \sigma(\mathbf{u}_h^k), \nabla_h \mathbf{m}_h)_{\omega_a} \quad (6.19)$$

with ∇_h denoting the standard broken gradient. Then, applying an integration by parts, using the properties of $\mathbf{M}_h^{\mathbf{a}}$, and the fact that, by definition, $\sigma_{h,\text{dis}}^{\mathbf{a},k} \in \Sigma_{h,\text{N,C,dis}}^{\mathbf{a},k}$, we obtain

$$\begin{aligned} (\sigma_{h,\text{dis}}^{\mathbf{a},k} - \psi_a \sigma(\mathbf{u}_h^k), \nabla_h \mathbf{m}_h)_{\omega_a} &= \sum_{T' \in \mathcal{T}_a} (\sigma_{h,\text{dis}}^{\mathbf{a},k} - \psi_a \sigma(\mathbf{u}_h^k), \nabla_h \mathbf{m}_h)_{T'} \\ &= - \underbrace{\sum_{T' \in \mathcal{T}_a} (\mathbf{div}(\sigma_{h,\text{dis}}^{\mathbf{a},k} - \psi_a \sigma(\mathbf{u}_h^k)), \mathbf{m}_h)_{T'}}_{=: \mathcal{I}_1} + \underbrace{\sum_{F \in \mathcal{F}_a^i} (\llbracket \psi_a \sigma(\mathbf{u}_h^k) \mathbf{n}_F \rrbracket, \mathbf{m}_h)_F}_{=: \mathcal{I}_2} \\ &\quad + \underbrace{\sum_{F \in \mathcal{F}_a^N} \left(\Pi_F^p(\psi_a \mathbf{g}_N) - \psi_a \sigma(\mathbf{u}_h^k) \mathbf{n}, \mathbf{m}_h \right)_F}_{=: \mathcal{I}_3} \\ &\quad + \underbrace{\sum_{F \in \mathcal{F}_a^C} \left(\Pi_F^p \left(\psi_a \left[\mathbf{P}_{1,\gamma}^n(\mathbf{u}_h^k) \right]_{\mathbb{R}^-} \right) - \psi_a \sigma^n(\mathbf{u}_h^k), \mathbf{m}_h^n \right)_F}_{=: \mathcal{I}_4} \\ &\quad + \underbrace{\sum_{F \in \mathcal{F}_a^C} \left(\Pi_F^p \left(\psi_a \left[\mathbf{P}_{1,\gamma}^t(\mathbf{u}_h^k) \right]_{S_h(\mathbf{u}_h^k)} \right) - \psi_a \sigma^t(\mathbf{u}_h^k), \mathbf{m}_h^t \right)_F}_{=: \mathcal{I}_5}. \end{aligned}$$

The first two terms can be treated as in [4, Proof of Theorem 4.7], obtaining

$$\begin{aligned} \mathcal{I}_1 &\lesssim \left[\sum_{T' \in \mathcal{T}_a} h_{T'}^2 \|\mathbf{div} \sigma(\mathbf{u}_h^k) + \Pi_{T'}^p \mathbf{f}\|_{T'}^2 \right]^{1/2} \|\nabla_h \mathbf{m}_h\|_{\omega_a}, \\ \mathcal{I}_2 &\lesssim \left[\sum_{F \in \mathcal{F}_a^i} h_F \|\llbracket \sigma(\mathbf{u}_h^k) \mathbf{n}_F \rrbracket\|_F^2 \right]^{1/2} \|\nabla_h \mathbf{m}_h\|_{\omega_a}. \end{aligned}$$

In a similar way, using the Cauchy–Schwarz inequality, the discrete trace inequality $\|\mathbf{m}_h\|_F \lesssim h_F^{-1/2} \|\mathbf{m}_h\|_{T'}$, and the discrete Poincaré inequality [28] when $\mathbf{a} \notin \mathcal{V}_h^D$ and the discrete Friedrichs inequality [28] when $\mathbf{a} \in \mathcal{V}_h^D$, together with the definition of $\mathbf{M}_h^{\mathbf{a}}$, we have

$$\begin{aligned}
\mathcal{I}_5 &= \sum_{F \in \mathcal{F}_a^C} \left(\psi_{\mathbf{a}} \left(\left[\mathbf{P}_{1,\gamma}^t(\mathbf{u}_h^k) \right]_{S_h(\mathbf{u}_h^k)} - \boldsymbol{\sigma}^t(\mathbf{u}_h^k) \right), \boldsymbol{\Pi}_F^p \mathbf{m}_h^t \right)_F \\
&= \sum_{F \in \mathcal{F}_a^C} \left(\boldsymbol{\Pi}_F^{p+1} \left[\mathbf{P}_{1,\gamma}^t(\mathbf{u}_h^k) \right]_{S_h(\mathbf{u}_h^k)} - \boldsymbol{\sigma}^t(\mathbf{u}_h^k), \psi_{\mathbf{a}} \boldsymbol{\Pi}_F^p \mathbf{m}_h^t \right)_F \\
&\leq \left[\sum_{F \in \mathcal{F}_a^C} h_F \left\| \psi_{\mathbf{a}} \left(\boldsymbol{\Pi}_F^{p+1} \left[\mathbf{P}_{1,\gamma}^t(\mathbf{u}_h^k) \right]_{S_h(\mathbf{u}_h^k)} - \boldsymbol{\sigma}^t(\mathbf{u}_h^k) \right) \right\|_F^2 \right]^{1/2} \left[\sum_{F \in \mathcal{F}_a^C} \frac{1}{h_F} \|\mathbf{m}_h\|_F^2 \right]^{1/2} \\
&\lesssim \left[\sum_{F \in \mathcal{F}_a^C} h_F \left\| \boldsymbol{\Pi}_F^{p+1} \left[\mathbf{P}_{1,\gamma}^t(\mathbf{u}_h^k) \right]_{S_h(\mathbf{u}_h^k)} - \boldsymbol{\sigma}^t(\mathbf{u}_h^k) \right\|_F^2 \right]^{1/2} \|\nabla_h \mathbf{m}_h\|_{\omega_a},
\end{aligned}$$

and also

$$\begin{aligned}
\mathcal{I}_3 &\lesssim \left[\sum_{F \in \mathcal{F}_a^N} h_F \left\| \boldsymbol{\Pi}_F^{p+1} \mathbf{g}_N - \boldsymbol{\sigma}(\mathbf{u}_h^k) \mathbf{n} \right\|_F^2 \right]^{1/2} \|\nabla_h \mathbf{m}_h\|_{\omega_a} \\
\mathcal{I}_4 &\lesssim \left[\sum_{F \in \mathcal{F}_a^C} h_F \left\| \boldsymbol{\Pi}_F^{p+1} \left(\left[P_{1,\gamma}(\mathbf{u}_h^k) \right]_{\mathbb{R}^-} \mathbf{n} \right) - \boldsymbol{\sigma}(\mathbf{u}_h^k) \mathbf{n} \right\|_F^2 \right]^{1/2} \|\nabla_h \mathbf{m}_h\|_{\omega_a}
\end{aligned}$$

Combining all the above results with (6.18) and (6.19) yields (6.17). \square

Remark 20 (Case $d = 3$). In the case $d = 3$, it becomes more challenging to identify a space similar to $\mathbf{M}_h^{\mathbf{a}}$ with the appropriate features to recover (6.19) and do the subsequent analysis. For this reason, in this paper, we present the proof of Lemma 19 specifically for the case $d = 2$.

Finally, (6.2) follows by combining the results of Lemmas 18 and 19, and (6.3) by using also the local stopping criterion (3.15).

6.2 Proof of the global efficiency

With the aim to prove (6.5) and (6.6) of Theorem 16 we introduce the global version of the local estimator $\eta_{\sharp,T}^k$:

$$\eta_{\sharp}^k := \left[\sum_{T \in \mathcal{T}_h} \left(\eta_{\sharp,T}^k \right)^2 \right]^{1/2}. \quad (6.20)$$

Lemma 21 (Control of the residual-based estimator η_{\sharp}^k). *Let $\mathbf{u}_h^k \in V_h$, let $\boldsymbol{\sigma}_h^k$ be the equilibrated stress defined by Construction 12, and let η_{\sharp}^k be the global residual-based estimator defined by (6.20). Then, for any $k \geq 1$*

$$\eta_{\sharp}^k \lesssim \|\mathcal{R}(\mathbf{u}_h^k)\|_* + \eta_{\text{osc}}^k + \eta_{\text{Neu}}^k + \eta_{\text{cnt}}^k + \eta_{\text{frc}}^k. \quad (6.21)$$

Proof. We have

$$\begin{aligned}
\eta_{\#}^k &\lesssim \underbrace{\left(\sum_{T \in \mathcal{T}_h} h_T^2 \|\mathbf{div} \boldsymbol{\sigma}(\mathbf{u}_h^k) + \boldsymbol{\Pi}_T^p \mathbf{f}\|_T^2 \right)^{1/2}}_{=: \mathcal{L}_1} + \underbrace{\left(\sum_{F \in \mathcal{F}_h^i} h_F \|\llbracket \boldsymbol{\sigma}(\mathbf{u}_h^k) \mathbf{n}_F \rrbracket\|_F^2 \right)^{1/2}}_{=: \mathcal{L}_2} + \\
&\quad + \underbrace{\left(\sum_{F \in \mathcal{F}_h^N} h_F \|\boldsymbol{\sigma}(\mathbf{u}_h^k) \mathbf{n} - \boldsymbol{\Pi}_F^{p+1} \mathbf{g}_N\|_F^2 \right)^{1/2}}_{=: \mathcal{L}_3} + \\
&\quad + \underbrace{\left(\sum_{F \in \mathcal{F}_h^C} h_F \|\boldsymbol{\sigma}^n(\mathbf{u}_h^k) - \boldsymbol{\Pi}_F^{p+1} [\mathbf{P}_{1,\gamma}^n(\mathbf{u}_h^k)]_{\mathbb{R}^-}\|_F^2 \right)^{1/2}}_{=: \mathcal{L}_4} + \\
&\quad + \underbrace{\left(\sum_{F \in \mathcal{F}_h^C} h_F \|\boldsymbol{\sigma}^t(\mathbf{u}_h^k) - \boldsymbol{\Pi}_F^{p+1} [\mathbf{P}_{1,\gamma}^t(\mathbf{u}_h^k)]_{S_h(\mathbf{u}_h^k)}\|_F^2 \right)^{1/2}}_{=: \mathcal{L}_5}
\end{aligned}$$

Proceeding as in the proof of Lemma 18, it is possible to show that

$$\begin{aligned}
\mathcal{L}_1 &\lesssim \|\mathcal{R}(\mathbf{u}_h^k)\|_* + \eta_{\text{osc}}^k, & \mathcal{L}_2 &\lesssim \|\mathcal{R}(\mathbf{u}_h^k)\|_* + \eta_{\text{osc}}^k, & \mathcal{L}_3 &\lesssim \|\mathcal{R}(\mathbf{u}_h^k)\|_* + \eta_{\text{osc}}^k + \eta_{\text{Neu}}^k, \\
\mathcal{L}_4 &\lesssim \|\mathcal{R}(\mathbf{u}_h^k)\|_* + \eta_{\text{osc}}^k + \eta_{\text{cnt}}^k, & \mathcal{L}_5 &\lesssim \|\mathcal{R}(\mathbf{u}_h^k)\|_* + \eta_{\text{osc}}^k + \eta_{\text{fric}}^k. & & \square
\end{aligned}$$

Lemma 22 (Control of the global stress estimator). *Let $\mathbf{u}_h^k \in \mathbf{V}_h$, let $\boldsymbol{\sigma}_h^k$ be the equilibrated stress defined by Construction 12, and let $\eta_{\#}^k$ be the global residual-based estimator defined by (6.20). Then, for any $k \geq 1$,*

$$\eta_{\text{str}}^k \lesssim \eta_{\#}^k.$$

Proof. It is an immediate consequence of Lemma 19. □

Finally, (6.5) follows by combining the results of Lemmas 21 and 22, and (6.6) by using also the global stopping criterion of Line 8 of Algorithm 1.

Acknowledgements

Funded by the European Union (ERC Synergy, NEMESIS, project number 101115663). Views and opinions expressed are however those of the author(s) only and do not necessarily reflect those of the European Union or the European Research Council Executive Agency. Neither the European Union nor the granting authority can be held responsible for them.

References

- [1] R. ARAYA AND F. CHOULY, *Residual a posteriori error estimation for frictional contact with Nitsche method*. 2023.

- [2] T. ARBOGAST AND Z. CHEN, *On the implementation of mixed methods as nonconforming methods for second-order elliptic problems*, *Mathematics of Computation*, 64 (1995), pp. 943–972.
- [3] D. N. ARNOLD, R. S. FALK, AND R. WINTHER, *Mixed finite element methods for linear elasticity with weakly imposed symmetry*, *Mathematics of Computation*, 76 (2007), pp. 1699–1723.
- [4] M. BOTTI AND R. RIEDLBECK, *Equilibrated stress tensor reconstruction and a posteriori error estimation for nonlinear elasticity*, *Computational Methods in Applied Mathematics*, 20 (2020), pp. 39–59.
- [5] D. CAPATINA AND R. LUCE, *Local flux reconstruction for a frictionless unilateral contact problem*, in *Numerical Mathematics and Advanced Applications ENUMATH 2019*, vol. 139 of *Lecture Notes in Computational Science and Engineering*, 2021, pp. 235–243.
- [6] F. CHOULY, *An adaptation of Nitsche’s method to the Tresca friction problem*, *Journal of Mathematical Analysis and Applications*, 411 (2014), pp. 329–339.
- [7] F. CHOULY, M. FABRE, P. HILD, R. MLIKA, J. POUSIN, AND Y. RENARD, *An overview of recent results on Nitsche’s method for contact problems*, *Geometrically Unfitted Finite Element Methods and Applications*, 121 (2017), pp. 93–141.
- [8] F. CHOULY, M. FABRE, P. HILD, J. POUSIN, AND Y. RENARD, *Residual-based a posteriori error estimation for contact problems approximated by Nitsche’s method*, *IMA Journal of Numerical Analysis*, 38 (2018), pp. 921–954.
- [9] F. CHOULY AND P. HILD, *A Nitsche-based method for unilateral contact problems: numerical analysis*, *SIAM Journal on Numerical Analysis*, 51 (2013), pp. 1295–1307.
- [10] ———, *Nitsche method for contact with Coulomb friction: Existence results for the static and dynamic finite element formulations*, *Journal of Computational and Applied Mathematics*, 416 (2022), p. 114557.
- [11] P. G. CIARLET, *The finite element method for elliptic problems*, vol. 40 of *Classics in Applied Mathematics*, Society for Industrial and Applied Mathematics (SIAM), Philadelphia, PA, 2002. Reprint of the 1978 original [North-Holland, Amsterdam; MR0520174 (58 #25001)].
- [12] A. CURNIER AND P. ALART, *A generalized Newton method for contact problems with friction*, *Journal de Mécanique Théorique et Appliquée*, 7 (1988), pp. 67–82.
- [13] D. A. DI PIETRO AND A. ERN, *Mathematical aspects of discontinuous Galerkin methods*, vol. 69 of *Mathématiques & Applications (Berlin) [Mathematics & Applications]*, Springer, Heidelberg, 2012.
- [14] D. A. DI PIETRO, I. FONTANA, AND K. KAZYMYRENKO, *A posteriori error estimates via equilibrated stress reconstructions for contact problems approximated by Nitsche’s method*, *Computers & Mathematics with Applications*, 111 (2022), pp. 61–80.
- [15] L. EL ALAOU, A. ERN, AND M. VOHRALÍK, *Guaranteed and robust a posteriori error estimates and balancing discretization and linearization errors for monotone nonlinear problems*, *Computer Methods in Applied Mechanics and Engineering*, 200 (2011), pp. 2782–2795.

- [16] A. ERN AND M. VOHRALÍK, *Polynomial-degree-robust a posteriori estimates in a unified setting for conforming, nonconforming, discontinuous galerkin, and mixed discretizations*, SIAM Journal on Numerical Analysis, 53 (2015), pp. 1058–1081.
- [17] I. FONTANA, *Modèles d’interface pour les ouvrages hydrauliques*, PhD thesis, Université de Montpellier, École doctorale Information Structures Systèmes, In preparation, 2022.
- [18] T. GUSTAFSSON, R. STENBERG, AND J. VIDEMAN, *On Nitsche’s method for elastic contact problems*, SIAM Journal on Scientific Computing, 42 (2020), pp. B425–B446.
- [19] J. HASLINGER, I. HLAVÁČEK, AND J. NEČAS, *Numerical methods for unilateral problems in solid mechanics*, in Finite Element Methods (Part 2), Numerical Methods for Solids (Part2), vol. 4 of Handbook of Numerical Analysis, Elsevier, 1996, pp. 313–485.
- [20] F. HECHT, *New development in FreeFem++*, J. Numer. Math., 20 (2012), pp. 251–265.
- [21] P. HILD AND V. LLERAS, *Residual error estimators for Coulomb friction*, SIAM Journal on Numerical Analysis, 47 (2009), pp. 3550–3583.
- [22] M. JUNTUNEN AND R. STENBERG, *Nitsche’s method for general boundary conditions*, Mathematics of computation, 78 (2009), pp. 1353–1374.
- [23] N. KIKUCHI AND Y. J. SONG, *Penalty/finite-element approximations of a class of unilateral problems in linear elasticity*, Quarterly of Applied Mathematics, 39 (1981), pp. 1–22.
- [24] J. NITSCHKE, *Über ein variationsprinzip zur lösung von Dirichlet-problemen bei verwendung von teilräumen, die keinen randbedingungen unterworfen sind*, Abhandlungen aus dem Mathematischen Seminar der Universität Hamburg, 36 (1971), pp. 9–15.
- [25] W. PRAGER AND J. L. SYNGE, *Approximations in elasticity based on the concept of function space*, Quart. Appl. Math., 5 (1947), pp. 241–269.
- [26] R. VERFÜRTH, *A review of a posteriori error estimation techniques for elasticity problems*, Computer Methods in Applied Mechanics and Engineering, 176 (1999), pp. 419–440.
- [27] R. VERFÜRTH, *A Review of A Posteriori Error Estimation and Adaptive Mesh-Refinement Techniques*, Wiley, June 1996.
- [28] M. VOHRALÍK, *On the discrete Poincaré-Friedrichs inequalities for nonconforming approximations of the Sobolev space H^1* , Numerical Functional Analysis and Optimization, 26 (2005), pp. 925–952.
- [29] ———, *A posteriori error estimates for efficiency and error control in numerical simulations*, UPMC Sorbonne Universités, February 2015.